5 Two texture zero neutrino mass in left-right symmetric model with $Z_8 \times Z_2$

In this chapter, we present a phenomenological study on the neutrino mass matrix M_ν favoring two zero texture in the framework of left-right symmetric model (LRSM) where type I and type II seesaw naturally occurs. The type I SS mass term is considered to be following a trimaximal mixing (TM) pattern. The symmetry realizations of these texture zero structures have been realized using the discrete cyclic abelian $Z_8 \times Z_2$ group in LRSM. We have studied six of the popular texture zero classes named as A1, A2, B1, B2, B3 and B4 favored by neutrino oscillation data in our analysis. We focused on the implications of these texture zero mass matrices in low energy phenomenon like neutrinoless double beta decay (NDBD) and lepton flavor violation (LFV) in the LRSM scenario. For NDBD, we have considered only the dominant new physics contribution coming from the diagrams containing purely RH current and another from the charged Higgs scalar while ignoring the contributions coming from the left-right gauge boson mixing and heavy light neutrino mixing. The mass of the extra gauge bosons and scalars has been considered to be of the order of TeV scale which is accessible at the colliders.

5.1 Introduction

Global analysis of neutrino oscillation data has quite precisely determined the best fit and 3σ ranges of neutrino parameters, viz., the mixing angles, mass squared differences, the Dirac CP phase δ [1], but the absolute neutrino mass and the additional CP phase (for Majorana

particles) α and β are not accurately found yet. Nevertheless, several other questions are yet not perceived amongst which notable is understanding the origin and dynamics of the neutrino mass and the lepton flavor structures of the fermions. The role of symmetry in particle physics [2] cannot be overestimated. It is utmost important to understand the underlying symmetry in order to understand the origin of the tiny neutrino mass and the large leptonic mixing. Symmetries can link two or more free parameters or can even make them vanish, thereby making the model more predictive. One of the possible role flavor symmetry can play is to impose texture zeros [3, 4, 5, 6, 7] in the mass matrix and to reduce the number of free parameters. For a symmetric M_ν, it has six independent complex entries. If n of them are considered to be vanishing, we arrive at ${}^6C_n = \frac{6!}{n!(6-n)!}$ different textures. A texture of $n \geqslant 3$ is not compatible with current experimental data and neutrino mixing angles. Texture zero approaches have been established as a feasible framework for explaining the fermion masses and mixing data in quark as well as lepton sector and has been studied in details in a large number of past works like [8, 9, 10, 11, 12, 13, 14, 15, 16]. Specifically, two texture zero mass matrices are considered to be more interesting as they can reduce the maximum number of free parameters. Two independent zeroes in the matrix can lead to four relations among the nine free parameters in the neutrino mass matrix which can be checked against the available experimental data.

In the simplest case, one can presume the charged lepton mass matrix to be diagonal and then consider the possible texture zeros in the symmetric Majorana mass matrix. Considering the basis in which charged lepton mass matrix is diagonal there are different categories of two zero texture neutrino mass matrix out of which some are ruled out and some are marginally allowed. Glashow et al.[4] have found seven acceptable textures of neutrino mass matrix (out of total fifteen) with two independent vanishing entries in the flavor basis for a diagonal charged lepton mass matrix to be consistent with current experimental data.

Neutrino mass and mixing matrix have different forms based upon some flavor symmetries. Amongst them, the most popular one which is consistent with neutrino oscillation data is the Tribimaximal mixing (TBM) [17] structure as proposed by Harison, Perkins and Scott. The resulting mass matrix in the basis of a diagonal charged lepton mass matrix is both 2-3 symmetric and magic. By magic, it means the row sums and column sums are all identical. The reactor mixing angle θ_{13} vanishes in TBM because of the bimaximal character of the

third mass eigenstate ν_3. However θ_{13} has been measured to be non-zero by experiments like T2K, Daya Bay, RENO and DOUBLE CHOOZ [18, 19, 20], which demands a correction to the TBM form which may be a correction or some perturbation to this type. Henceforth, owing to the current scenario of neutrino oscillation parameters several new models have been theorized and studied by the scientific communities. Amongst several neutrino mass models, Trimaximal mixing (TM) [21, 22, 23, 24, 25, 26, 27, 28] is one in which non-zero reactor mixing angle can be realized. The mixing matrix consists of identical second column elements similar to the TBM type. However, it relaxes some of the TBM assumptions, since it allows for a non-zero θ_{13} as well as preserves the solar mixing angle prediction. Besides the zeros in the neutrino mass matrix which is one of currently studied approaches for precisely explaining neutrino masses and mixing can also be examined using the TM mixing.

As we have mentioned in the earlier chapters that one of the important processes which undoubtedly establishes the Majorana nature of neutrinos (violation of lepton number by two units) is neutrinoless double beta decay (NDBD) (for a review see[29]). Besides, the observation of NDBD would also throw light on the absolute scale of neutrino mass and in explaining the matter-antimatter asymmetry of the universe. The NDBD experiments like KamLAND-Zen, GERDA, EXO-200 [30, 31, 32] directly measures and provides bounds on the decay half-life which can be converted to the effective neutrino mass parameter, m_{ee} with certain uncertainty which arises due to the theoretical uncertainty in the NME. The current best limits on the effective mass $< m_{ee} >$ are of the order of 100 meV. The next-generation experiments target to increase the sensitivity in the 10 meV mass range. Thus, future NDBD experiments can shed lights on several issues in the neutrino sector. Observing this rare decay process with the current experiments would signify new physics contributions beyond the Standard Model (BSM) other than the standard light neutrino contribution.

There are several BSM frameworks, amongst which one of the most fascinating and modest frameworks in which neutrino mass and other unsolved queries can be addressed is the left right symmetric model (LRSM) [33, 34, 35]. It has become a topic of interest since long back owing to its indomitable importance and has been studied in details by several groups in different contexts [36, 37, 38, 39, 40, 41, 42, 43, 44, 45, 46]. As far as NDBD is concerned, LRSM can give rise to several new physics (non-standard) contributions coming from LH,

RH, mixed, scalar triplet etc. Several analysis has been done already involving NDBD in LRSM [39, 42, 40, 41, 42, 43, 44, 45] and their compatibility with LHC experiments [47, 48, 49, 50, 40].

As cited by several authors [28, 27], the TM mixing can satisfy the current neutrino experimental data when combined with two zero textures. In this context, we have done a phenomenological study on the neutrino mass matrix M_ν favoring two zero texture in the framework of LRSM where type I and type II seesaw naturally occurs. The type I SS mass term is considered to be following a TM mixing pattern. The symmetry realizations of these texture zero structures has been realized using the discrete cyclic abelian ($Z_8 \times Z_2$) group in LRSM. In order to obtain the desired two zero textures of the mass matrices, we have added two more LH and RH scalar triplets each. In our analysis, we have studied for the popular 6 texture zero classes being named as A1-A2 and B1-B4. We basically focused in the implications of these texture zero mass matrices in low energy phenomenon like NDBD and LFV in LRSM scenario. For NDBD, we have considered only the dominant new physics contribution coming from the diagrams containing purely RH current mediated by the heavy gauge boson, W_R by the exchange of heavy right-handed (RH) neutrino, N_R and another from the charged Higgs scalars mediated by the heavy gauge boson W_R ignoring the contributions coming from the left-right gauge boson mixing and heavy light neutrino mixing as in chapter 5. The mass of the extra gauge bosons and scalars has been considered to be of the order of TeV accessible at the colliders.

This chapter has been organized as follows, in the next section we briefly review two texture zero and TM mixing. In section 5.3 we present the symmetry realizations of these classes by using a cyclic $Z_8 \times Z_2$ group symmetry with possible particle contents in LRSM to obtain the desired texture zero matrices. Then in section 5.4 we discuss NDBD and LFV in the framework of LRSM which is followed by the numerical analysis and results with the collider signatures in section 5.5. We give the conclusion in section 5.6.

5.2 Two zero texture and tri-maximal mixing

Non-vanishing θ_{13} excluded $\mu - \tau$ symmetry to be an exact symmetry of the neutrino mass matrix which opts for a perturbation in $\mu - \tau$ symmetric mass matrix or a different form which gives rise to non-zero θ_{13}. Going through literature, we have seen that another form of symmetry known as magic symmetry can serve the purpose [51]. The corresponding mass matrix known as the magic symmetric mass matrix can be made more predictive by imposing certain constraints in it. Adding zeroes in certain elements of the matrix can make it more anticipating. One zero and two zero textures of certain types in neutrino mass matrix are consistent with the neutrino data. We here study two zero texture in neutrino mass matrix M_ν which was first considered in [4, 5] and subsequently by several other groups [52, 11, 10, 12, 53, 6, 7, 8, 13, 14]. Trimaximal mixing (TM) in two texture zero has been extensively studied in literature [28, 27]. In TM, $\mu - \tau$ symmetry is broken but the magic symmetry is kept intact. It has been again named as TM_1 or TM_2 based upon whether the second or the first column of the TBM mixing matrix remains intact respectively. We have studied these allowed texture zeros in the magic neutrino mass matrix (satisfying TM_2 mixing) which is the type I SS mass term in our case and studied its implications for low energy processes like NDBD and LFV. Two zero textures ensure two independent vanishing entries in the neutrino mass matrix. There are a total of ${}^6C_2$ i.e., 15 texture zeros of Mν which has been further classified into 6 subcategories and can be named as- A1, A2; B1, B2, B3, B4; C1; D1, D2; E1, E2, E3; F1, F2, F3. Out of the above, E1-E3; F1-F3 were ruled out, D1, D2 are marginally allowed and now has been experimentally ruled out at 3σ level. We are only left with 7 allowed cases of 2 zero textures, viz., A1-A2; B1-B4 and C1, we are concerned with six of the above classes which are of the form,

$$A1 = \begin{bmatrix} 0 & 0 & X \\ 0 & X & X \\ X & X & X \end{bmatrix}, A2 = \begin{bmatrix} 0 & X & 0 \\ X & X & X \\ 0 & X & X \end{bmatrix}, B1 = \begin{bmatrix} X & X & 0 \\ X & 0 & X \\ 0 & X & X \end{bmatrix} \tag{5.1}$$

$$B2 = \begin{bmatrix} X & 0 & X \\ 0 & X & X \\ 0 & X & 0 \end{bmatrix}, B3 = \begin{bmatrix} X & 0 & X \\ 0 & 0 & X \\ X & X & X \end{bmatrix}, B4 = \begin{bmatrix} X & X & 0 \\ X & X & X \\ 0 & X & 0 \end{bmatrix} \tag{5.2}$$

The neutrino mass matrix is said to be invariant under a magic symmetry and the corresponding mixing symmetry is known as trimaximal mixing (TM) with the TM_2 mixing matrix given by,

$$U_{TM2} = \begin{bmatrix} \sqrt{\frac{2}{3}}cos\theta & \frac{1}{\sqrt{3}} & \sqrt{\frac{2}{3}}sin\theta \\ -\frac{cos\theta}{\sqrt{6}} + \frac{e^{-i\phi}sin\theta}{\sqrt{2}} & \frac{1}{\sqrt{3}} & -\frac{sin\theta}{\sqrt{6}} - \frac{e^{-i\phi}cos\theta}{\sqrt{2}} \\ -\frac{cos\theta}{\sqrt{6}} - \frac{e^{-i\phi}sin\theta}{\sqrt{2}} & \frac{1}{\sqrt{3}} & -\frac{sin\theta}{\sqrt{6}} + \frac{e^{-i\phi}cos\theta}{\sqrt{2}} \end{bmatrix}, \tag{5.3}$$

where θ and ϕ being the free parameters. It diagonalizes the magic neutrino mass matrix, which can be parameterized as,

$$M_{magic} = \begin{bmatrix} p & q & r \\ q & r & p+r-s \\ r & p+r-s & q-r+s \end{bmatrix} \tag{5.4}$$

The different allowed classes of two zero texture along with their respective constraint equations are as shown in table 5.1 Using these constraint equations, we can arrive at the different

$Class$	Constraint equations
A_1	$M_{ee} = 0, M_{e\mu} = 0$
A_2	$M_{ee} = 0, M_{e\tau} = 0$
B_1	$M_{e\tau} = 0, M_{\mu\mu} = 0$
B_2	$M_{e\mu} = 0, M_{\tau\tau} = 0$
B_3	$M_{e\mu} = 0, M_{\mu\mu} = 0$
B_4	$M_{\mu\mu} = 0, M_{\tau\tau} = 0$

Table 5.1: Constraint relations for two texture zero mass matrix.

classes of two zero textured neutrino mass matrix favouring TM_2 mixing.

5.3 Symmetry realizations in LRSM

The light neutrino mass in LRSM generated within a type I+II seesaw is,

$$M_\nu = M_{LL} - M_D {M_{RR}}^{-1} {M_D}^T = \sqrt{2} v_L f_L - \frac{v_{\rm SM}^2}{\sqrt{2} v_R} h_D {f_R}^{-1} {h_D}^T, \tag{5.5}$$

$$M_D = \frac{1}{\sqrt{2}}(k_1 h + k_2 \tilde{h}), M_{LL} = \sqrt{2} v_L f_L, M_{RR} = \sqrt{2} v_R f_R, \tag{5.6}$$

$$\mathrm{h_D} = \frac{(\mathrm{k_1 h} + \mathrm{k_2 \tilde{h}})}{\sqrt{2}\mathrm{v_{SM}}}. \tag{5.7}$$

M_D, M_{LL} and M_{RR} being the Dirac neutrino mass matrix, LH and RH Majorana mass matrix respectively. The first and second terms in equation (5.5) correspond to type II seesaw and type I seesaw contributions respectively. Several earlier works [52, 11, 10, 12, 53, 6, 7, 8, 13, 14] has explained two zero texture which has been explored BSM to address neutrino masses and mixing. In this work, we have extended the minimal left-right symmetric model by introducing two more LH and RH scalar triplets represented by $\Delta_L{}', \Delta_L{}''$ and $\Delta_R{}', \Delta_R{}''$ respectively for the classes B1-B4 and three more for the classes A1 and A2 ($\Delta_L{}', \Delta_L{}'', \Delta_L{}'''$ and $\Delta_R{}', \Delta_R{}'', \Delta_R{}'''$) to realize the desired textures of Dirac and Majorana mass matrix, M_D and M_{RR} while keeping in mind that the charged lepton mass matrix is diagonal. The symmetry realizations of these texture zero structures has been worked out using the discrete abelian ($Z_8 \times Z_2$) group in the framework of LRSM which are explained below.

Class A1:

The symmetry realization for the class A1 is shown in tabular form as below,

l_L	$Z_8 \times Z_2$	l_R	$Z_8 \times Z_2$	$\Delta(LH)$	$Z_8 \times Z_2$	$\Delta(RH)$	$Z_8 \times Z_2$
l_{Le}	$(\omega^4, 1)$	l_{Re}	$(\omega^4, 1)$	Δ_L	$(\omega^2, -1)$	Δ_R	$(1, 1)$
$l_{L\mu}$	$(\omega^3, -1)$	$l_{R\mu}$	$(\omega^5, -1)$	$\Delta_L{}'$	$(\omega^2, 1)$	$\Delta_R{}'$	$(\omega^7, -1)$
$l_{L\tau}$	$(\omega^2, -1)$	$l_{R\tau}$	$(\omega^6, -1)$	$\Delta_L{}''$	$(\omega^3, 1)$,	$\Delta_R{}''$	$(\omega^6, -1)$
				$\Delta_L{}'''$	$(\omega^4, 1)$,	$\Delta_R{}'''$	$(\omega^6, 1)$

Table 5.2: Particle assignments for A1

In the classes A1 and A2, the bidoublets ϕ and $\tilde{\phi}$ transforms as singlets (1×1) under the cyclic group $Z_8 \times Z_2$. The diagonal Dirac and the charged lepton mass term(which is same for all the cases), in the matrix form can be written as,

$$M_D = \begin{bmatrix} 1 & \omega^3 & \omega^3 \\ \omega^5 & 1 & -1 \\ \omega^5 & -1 & 1 \end{bmatrix} + \begin{bmatrix} 1 & \omega^3 & \omega^3 \\ \omega^5 & 1 & -1 \\ \omega^5 & -1 & 1 \end{bmatrix} \simeq \begin{bmatrix} \times & 0 & 0 \\ 0 & \times & 0 \\ 0 & 0 & \times \end{bmatrix} \tag{5.8}$$

The corresponding Dirac Yukawa Lagrangian for A1 and A2 can be written as,

$$\mathcal{L}_{\mathcal{D}} = Y_{ee}\overline{L}_{Le}\phi\overline{L}_{Re} + \tilde{Y_{ee}}\overline{L}_{Le}\tilde{\phi}\overline{L}_{Re} + Y_{\mu\mu}\overline{L}_{L\mu}\phi\overline{L}_{R\mu} + \tilde{Y_{\mu\mu}}\overline{L}_{L\mu}\tilde{\phi}\overline{L}_{R\mu} + Y_{\tau\tau}\overline{L}_{L\tau}\phi\overline{L}_{R\tau} + \tilde{Y_{\tau\tau}}\overline{L}_{L\tau}\tilde{\phi}\overline{L}_{R\tau} \tag{5.9}$$

Under these symmetry realizations, we get the Majorana mass terms (LH and RH) and the type I SS mass terms for the class A1, in the matrix form as,

$$M_{RR} = \begin{bmatrix} 1 & 1 & 1 \\ 1 & 1 & \omega^3 \\ 1 & \omega^3 & \omega^4 \end{bmatrix}, M_{LL} = \begin{bmatrix} \omega^2 & 0 & 1 \\ 0 & 1 & 1 \\ 1 & 1 & 1 \end{bmatrix}, M^I = \begin{bmatrix} 0 & 0 & \times \\ 0 & \times & \times \\ \times & \times & \times \end{bmatrix} \tag{5.10}$$

The Majorana Yukawa Lagrangian (LH and RH) for A1 is thus given as,

$$\mathcal{L}_{\mathcal{MR}} = Y_{Ree}{L_{Re}}^T\Delta_R L_{Re} + Y_{Re\mu}{L_{Re}}^T\Delta_R^{'}L_{R\mu} + Y_{R\mu e}{L_{R\mu}}^T{\Delta_R}^{'}L_{Re} + Y_{Re\tau}{L_{Re}}^T{\Delta_R}^{''}L_{R\tau} + Y_{R\tau e}{L_{R\tau}}^T{\Delta_R}^{''}L_{Re} + Y_{R\mu\mu}{L_{R\mu}}^T{\Delta_R}^{'''}L_{R\mu}. \tag{5.11}$$

$$\mathcal{L}_{\mathcal{ML}} = Y_{Le\tau}{L_{Le}}^T\Delta_L L_{L\tau} + Y_{L\tau e}{L_{L\tau}}^T\Delta_L L_{Le} + Y_{L\mu\mu}{L_{L\mu}}^T{\Delta_L}^{'}L_{L\mu} + Y_{L\mu\tau}{L_{L\mu}}^T{\Delta_L}^{''}L_{L\tau} + Y_{L\tau\mu}{L_{L\tau}}^T{\Delta_L}^{''}L_{L\mu} + Y_{L\tau\tau}{L_{L\tau}}^T{\Delta_L}^{'''}L_{L\tau}. \tag{5.12}$$

Class A2:

For the class A2, to get the desired texture zero structures for the mass matrices, the following symmetry realization has been adopted.

l_L	$Z_8 \times Z_2$	l_R	$Z_8 \times Z_2$	$\Delta(LH)$	$Z_8 \times Z_2$	$\Delta(RH)$	$Z_8 \times Z_2$
l_{Le}	$(\omega^4, 1)$	l_{Re}	$(\omega^4, 1)$	Δ_L	$(\omega, -1)$	Δ_R	$(1, 1)$
$l_{L\mu}$	$(\omega^3, -1)$	$l_{R\mu}$	$(\omega^5, -1)$	${\Delta_L}^{'}$	$(\omega^2, 1)$	${\Delta_R}^{'}$	$(\omega^7, -1)$
$l_{L\tau}$	$(\omega^2, -1)$	$l_{R\tau}$	$(\omega^6, -1)$	${\Delta_L}^{''}$	$(\omega^3, 1)$,	${\Delta_R}^{''}$	$(\omega^6, -1)$
				${\Delta_L}^{'''}$	$(\omega^4, 1)$,	${\Delta_R}^{'''}$	$(\omega^4, 1)$

Table 5.3: Particle assignments for A2

The Majorana mass terms (LH and RH) and the type I SS mass terms, in the matrix form

has been obtained as,

$$M_{RR} = \begin{bmatrix} 1 & 1 & 1 \\ 1 & \omega^2 & \omega^3 \\ 1 & \omega^3 & 1 \end{bmatrix}, M_{LL} = \begin{bmatrix} \omega & 1 & \omega^7 \\ 1 & 1 & 1 \\ \omega^7 & 1 & 1 \end{bmatrix}, M^I = \begin{bmatrix} 0 & \times & 0 \\ \times & \times & \times \\ 0 & \times & \times \end{bmatrix}. \tag{5.13}$$

The corresponding Majorana Yukawa Lagrangian (LH and RH) for A2 is,

$$\begin{aligned} \mathcal{L}_{\mathcal{MR}} = Y_{Re\mu} L_{Re}{}^T \Delta_R L_{R\mu} + Y_{R\mu e} L_{R\mu}{}^T \Delta_R L_{Re} + Y_{R\mu\mu} L_{R\mu}{}^T \Delta_R{}' L_{R\mu} + \\ Y_{R\mu\tau} L_{R\mu}{}^T \Delta_R{}'' L_{R\tau} + Y_{R\tau\mu} L_{R\tau}{}^T \Delta_R{}'' L_{R\mu} + Y_{R\tau\tau} L_{R\tau}{}^T \Delta_R{}' L_{R\tau} \end{aligned} \tag{5.14}$$

$$\begin{aligned} \mathcal{L}_{\mathcal{ML}} = Y_{Le\mu} L_{Le}{}^T \Delta_L L_{L\mu} + Y_{L\mu e} L_{L\mu}{}^T \Delta_L L_{Le} + Y_{L\mu\mu} L_{L\mu}{}^T \Delta_L{}' L_{L\mu} + \\ Y_{L\mu\tau} L_{L\mu}{}^T \Delta_L{}'' L_{L\tau} + Y_{L\tau\mu} L_{L\tau}{}^T \Delta_L{}'' L_{L\mu} + Y_{L\tau\tau} L_{L\tau}{}^T \Delta_L{}''' L_{L\tau} \end{aligned} \tag{5.15}$$

Class B1: The symmetry realizations of the particles under $Z8 \times Z2$ for the class B1 are as shown in the table 5.4. In the classes B1 to B4, the bidoublets ϕ and $\tilde{\phi}$ transforms as

l_L	$Z_8 \times Z_2$	l_R	$Z_8 \times Z_2$	$\Delta(LH)$	$Z_8 \times Z_2$	$\Delta(RH)$	$Z_8 \times Z_2$
l_{Le}	$(\omega^2, 1)$	l_{Re}	$(\omega^6, 1)$	Δ_L	$(\omega^4, 1)$	Δ_R	$(\omega^4, 1)$
$l_{L\mu}$	$(\omega^3, -1)$	$l_{R\mu}$	$(\omega^5, -1)$	$\Delta_L{}'$	$(\omega^3, -1)$	$\Delta_R{}'$	$(\omega^5, -1)$
$l_{L\tau}$	$(\omega^3, -1)$	$l_{R\tau}$	$(\omega^5, -1)$	$\Delta_L{}''$	$(\omega^2, 1)$	$\Delta_R{}''$	$(\omega^6, 1)$

Table 5.4: Particle assignments for B1

$\phi \to (1,1)\phi$, $\phi' \to (1,-1)\phi'$ under the cyclic group $Z_8 \times Z_2$. The diagonal Dirac and the charged lepton mass term for B1 to B4 are given by,

$$M_D = \begin{bmatrix} 1 & \omega^7 & \omega^7 \\ \omega & 1 & -1 \\ \omega & -1 & 1 \end{bmatrix} + \begin{bmatrix} 1 & \omega^7 & \omega^7 \\ \omega & 1 & -1 \\ \omega & -1 & 1 \end{bmatrix} \simeq \begin{bmatrix} \times & 0 & 0 \\ 0 & \times & 0 \\ 0 & 0 & \times \end{bmatrix} \tag{5.16}$$

The corresponding Dirac Yukawa Lagrangian for B1 to B4 can be written as,

$$\begin{aligned} \mathcal{L}_{\mathcal{D}} = Y_{ee} \overline{L}_{Le} \phi \overline{L}_{Re} + \tilde{Y_{ee}} \overline{L}_{Le} \tilde{\phi} \overline{L}_{Re} + Y_{\mu\mu} \overline{L}_{L\mu} \phi \overline{L}_{R\mu} + \tilde{Y_{\mu\mu}} \overline{L}_{L\mu} \tilde{\phi} \overline{L}_{R\mu} + \\ Y_{\tau\tau} \overline{L}_{L\tau} \phi \overline{L}_{R\tau} + \tilde{Y_{\tau\tau}} \overline{L}_{L\tau} \tilde{\phi} \overline{L}_{R\tau} \end{aligned} \tag{5.17}$$

These transformations leads to the Majorana mass matrices (LH and RH) as,

$$M_{RR} = \begin{bmatrix} 1 & 1 & 1 \\ 1 & 1 & 1 \\ 1 & 1 & 1 \end{bmatrix}, M_{LL} = \begin{bmatrix} 1 & 1 & \omega^4 \\ 1 & \omega & 1 \\ \omega^4 & 1 & 1 \end{bmatrix}, M^I = \begin{bmatrix} \times & \times & 0 \\ \times & 0 & \times \\ 0 & \times & \times \end{bmatrix} \tag{5.18}$$

The corresponding $Z8 \times Z2$ invariant Majorana Yukawa Lagrangian (LH and RH) for B1 is,

$$\begin{aligned} \mathcal{L}_{\mathcal{MR}} = Y_{Ree} {L_{Re}}^T \Delta_R L_{Re} + Y_{Re\mu} {L_{Re}}^T {\Delta_R}' L_{R\mu} + Y_{R\mu e} {L_{R\mu}}^T {\Delta_R}' L_{Re} + \\ Y_{Re\tau} {L_{Re}}^T \Delta_R L_{R\tau} + Y_{R\tau e} {L_{R\tau}}^T \Delta_R L_{Re} + Y_{R\mu\mu} {L_{R\mu}}^T {\Delta_R}'' L_{R\mu} \\ + Y_{R\mu\tau} {L_{R\mu}}^T {\Delta_R}'' L_{R\tau} + Y_{R\tau\mu} {L_{R\tau}}^T {\Delta_R}'' L_{R\mu} Y_{R\tau\tau} {L_{R\tau}}^T {\Delta_R}'' L_{R\tau}. \end{aligned} \tag{5.19}$$

$$\begin{aligned} \mathcal{L}_{\mathcal{ML}} = Y_{Lee} {L_{Le}}^T \Delta_L L_{Le} + Y_{Le\mu} {L_{Le}}^T \Delta_L L_{R\mu} + Y_{L\mu e} {L_{L\mu}}^T {\Delta_L}' L_{Le} + \\ Y_{L\mu\tau} {L_{L\mu}}^T {\Delta_L}' L_{L\tau} + Y_{L\tau\mu} {L_{L\tau}}^T {\Delta_L}'' L_{L\mu} + Y_{L\tau\tau} {L_{L\tau}}^T {\Delta_L}'' L_{L\tau}. \end{aligned} \tag{5.20}$$

Class B2: The symmetry realizations to obtain the desired textures of the class B1 are as shown in the table 5.5,

l_L	$Z_8 \times Z_2$	l_R	$Z_8 \times Z_2$	$\Delta(LH)$	$Z_8 \times Z_2$	$\Delta(RH)$	$Z_8 \times Z_2$
l_{Le}	$(\omega^2, 1)$	l_{Re}	$(\omega^6, 1)$	Δ_L	$(\omega^4, 1)$	Δ_R	$(\omega^4, 1)$
$l_{L\mu}$	$(\omega^3, -1)$	$l_{R\mu}$	$(\omega^5, -1)$	${\Delta_L}'$	$(\omega^3, -1)$	${\Delta_R}'$	$(\omega^5, -1)$
$l_{L\tau}$	$(\omega^3, -1)$	$l_{R\tau}$	$(\omega^5, -1)$	${\Delta_L}''$	$(\omega^2, 1)$	${\Delta_R}''$	$(\omega^6, 1)$

Table 5.5: Particle assignments for B2

The Majorana mass matrices (LH and RH) and the type I SS mass matrix under these transformation has been obtained as,

$$M_{RR} = \begin{bmatrix} 1 & 1 & 1 \\ 1 & 1 & 1 \\ 1 & 1 & 1 \end{bmatrix}, M_{LL} = \begin{bmatrix} 1 & \omega & 1 \\ \omega & 1 & 1 \\ 1 & 1 & \omega^2 \end{bmatrix}, M^I = \begin{bmatrix} \times & 0 & \times \\ 0 & \times & \times \\ \times & \times & 0 \end{bmatrix} \tag{5.21}$$

The corresponding Majorana Yukawa Lagrangian (LH and RH) for the class B2 is,

$$\begin{aligned} \mathcal{L}_{\mathcal{MR}} = Y_{Ree} {L_{Re}}^T \Delta_R L_{Re} + Y_{Re\mu} {L_{Re}}^T \Delta_R^{'} L_{R\mu} + Y_{R\mu e} {L_{R\mu}}^T {\Delta_R}' L_{Re} + \\ Y_{Re\tau} {L_{Re}}^T \Delta_R^{'} L_{R\tau} + Y_{R\tau e} {L_{R\tau}}^T {\Delta_R}' L_{Re} + Y_{R\mu\mu} {L_{R\mu}}^T {\Delta_R}'' L_{R\mu} \\ + Y_{R\mu\tau} {L_{R\mu}}^T {\Delta_R}'' L_{R\tau} + Y_{R\tau\mu} {L_{R\tau}}^T {\Delta_R}'' L_{R\mu} + Y_{R\tau\tau} {L_{R\tau}}^T {\Delta_R}'' L_{R\tau} \end{aligned} \tag{5.22}$$

$$\begin{aligned}\mathcal{L}_{\mathcal{ML}} = Y_{Lee} {L_{Le}}^T \Delta_L L_{Le} + Y_{Le\tau} {L_{Le}}^T \Delta_L^{'} L_{L\tau} + Y_{L\tau e} {L_{L\tau}}^T {\Delta_L}^{'} L_{Le} + \\ Y_{L\mu\mu} {L_{L\mu}}^T {\Delta_L}^{''} L_{L\mu} + Y_{L\mu\tau} {L_{L\mu}}^T {\Delta_L}^{''} L_{L\tau} + Y_{L\tau\mu} {L_{L\tau}}^T {\Delta_L}^{''} L_{L\mu}\end{aligned} \tag{5.23}$$

Class B3: The symmetry realizations of the particles to obtain the desired mass terms of class B3 is shown in table 5.6.

l_L	$Z_8 \times Z_2$	l_R	$Z_8 \times Z_2$	$\Delta(LH)$	$Z_8 \times Z_2$	$\Delta(RH)$	$Z_8 \times Z_2$
l_{Le}	$(\omega^2, 1)$	l_{Re}	$(\omega^6, 1)$	Δ_L	$(\omega^4, 1)$	Δ_R	$(\omega^4, 1)$
$l_{L\mu}$	$(\omega^3, -1)$	$l_{R\mu}$	$(\omega^5, -1)$	${\Delta_L}^{'}$	$(\omega^3, -1)$	${\Delta_R}^{'}$	$(\omega^5, -1)$
$l_{L\tau}$	$(\omega^3, -1)$	$l_{R\tau}$	$(\omega^5, -1)$	${\Delta_L}^{''}$	$(\omega^2, 1)$	${\Delta_R}^{''}$	$(\omega^6, 1)$

Table 5.6: Particle assignments for B3

The Majorana mass terms (LH and RH) and the type I SS mass terms, in the matrix form can be written as,

$$M_{RR} = \begin{bmatrix} 1 & 1 & \omega^7 \\ 1 & 1 & 1 \\ \omega^7 & 1 & \omega^6 \end{bmatrix}, M_{LL} = \begin{bmatrix} 1 & \omega & 1 \\ \omega & \omega^2 & 1 \\ 1 & 1 & 1 \end{bmatrix}, M^I = \begin{bmatrix} \times & 0 & \times \\ 0 & 0 & \times \\ \times & \times & \times \end{bmatrix} \tag{5.24}$$

The corresponding Majorana Yukawa Lagrangian (LH and RH) for B3 is,

$$\begin{aligned}\mathcal{L}_{\mathcal{MR}} = Y_{Ree} {L_{Re}}^T \Delta_R L_{Re} + Y_{Re\mu} {L_{Re}}^T \Delta_R^{'} L_{R\mu} + Y_{R\mu e} {L_{R\mu}}^T \Delta_R^{'} L_{Re} + \\ Y_{R\mu\mu} {L_{R\mu}}^T {\Delta_R}^{''} L_{R\mu} + Y_{R\mu\tau} {L_{R\mu}}^T {\Delta_R}^{''} L_{R\tau} + Y_{R\tau\mu} {L_{R\tau}}^T {\Delta_R}^{''} L_{R\mu}\end{aligned} \tag{5.25}$$

$$\begin{aligned}\mathcal{L}_{\mathcal{ML}} = Y_{Lee} {L_{Le}}^T \Delta_L L_{Le} + Y_{Le\tau} {L_{Le}}^T {\Delta_L}^{'} L_{L\tau} + Y_{L\tau e} {L_{L\tau}}^T {\Delta_L}^{'} L_{Le} + \\ Y_{L\mu\tau} {L_{L\mu}}^T {\Delta_L}^{''} L_{L\tau} + Y_{L\tau\mu} {L_{L\tau}}^T {\Delta_L}^{''} L_{L\mu} + Y_{L\tau\tau} {L_{L\tau}}^T {\Delta_L}^{''} L_{L\tau}\end{aligned} \tag{5.26}$$

Class B4:

Similarly, we give the transformations for the class B4 as shown in table 5.7 to obtain the desired texture zero mass matrices.

l_L	$Z_8 \times Z_2$	l_R	$Z_8 \times Z_2$	$\Delta(LH)$	$Z_8 \times Z_2$	$\Delta(RH)$	$Z_8 \times Z_2$
l_{Le}	$(\omega^2, 1)$	l_{Re}	$(\omega^6, 1)$	Δ_L	$(\omega^4, 1)$	Δ_R	$(\omega^4, 1)$
$l_{L\mu}$	$(\omega^3, -1)$	$l_{R\mu}$	$(\omega^5, -1)$	$\Delta_L{}'$	$(\omega^3, -1)$	$\Delta_R{}'$	$(\omega^5, -1)$
$l_{L\tau}$	$(\omega^3, -1)$	$l_{R\tau}$	$(\omega^5, -1)$	$\Delta_L{}''$	$(\omega^2, 1)$	$\Delta_R{}''$	$(\omega^6, 1)$

Table 5.7: Particle assignments for B4

Under these symmetry realizations, we obtain the Majorana mass terms (LH and RH) and the type I SS mass terms as,

$$M_{RR} = \begin{bmatrix} 1 & \omega^7 & 1 \\ \omega^7 & \omega^6 & 1 \\ 1 & 1 & 1 \end{bmatrix}, M_{LL} = \begin{bmatrix} 1 & 1 & \omega \\ 1 & 1 & 1 \\ \omega & 1 & \omega^4 \end{bmatrix}, M^I = \begin{bmatrix} \times & \times & 0 \\ \times & \times & \times \\ 0 & \times & 0 \end{bmatrix} \tag{5.27}$$

The Majorana Yukawa Lagrangian (LH and RH) for B4 thus becomes,

$$\begin{aligned} \mathcal{L}_{\mathcal{MR}} = Y_{Ree} L_{Re}{}^T \Delta_R L_{Re} + Y_{Re\tau} L_{Re}{}^T \Delta_R{}'' L_{R\tau} + Y_{R\tau e} L_{R\tau}{}^T \Delta_R{}'' L_{Re} + \\ Y_{R\mu\tau} L_{R\mu}{}^T \Delta_R{}'' L_{R\tau} + Y_{R\tau\mu} L_{R\tau}{}^T \Delta_R{}' L_{R\mu} + Y_{R\tau\tau} L_{R\tau}{}^T \Delta_R{}'' L_{R\tau} \end{aligned} \tag{5.28}$$

$$\begin{aligned} \mathcal{L}_{\mathcal{ML}} = Y_{Lee} L_{Le}{}^T \Delta_L L_{Le} + Y_{Le\mu} L_{Le}{}^T \Delta_L{}' L_{L\mu} + Y_{L\mu e} L_{L\mu}{}^T \Delta_L{}' L_{Le} + \\ Y_{L\mu\mu} L_{L\mu}{}^T \Delta_L{}'' L_{L\mu} + Y_{L\mu\tau} L_{L\mu}{}^T \Delta_L{}'' L_{L\tau} + Y_{L\tau\mu} L_{L\tau}{}^T \Delta_L{}'' L_{L\mu} \end{aligned} \tag{5.29}$$

LRSM being a combination of type I and type II SS mass terms would give us the final mass matrix that would obey the structure of two zero texture mass matrix. It has been shown in tabular form in the numerical analysis.

5.4 Neutrinoless double beta decay and lepton flavor violation in LRSM.

The very facts of LRSM and the presence of several new heavy particles leads to many new contributions to NDBD apart from the standard light neutrino contribution. This has been extensively studied in several earlier works [39, 42, 40, 41, 42, 43, 44, 45]. Amongst the non-standard contribution, notable are heavy RH neutrino contribution to NDBD in which

the mediator particles are the $W_L{}^-$ and $W_R{}^-$ boson individually, light neutrino contribution to NDBD in which the intermediate particles are $W_R{}^-$ bosons, light neutrino contribution mediated by both $W_L{}^-$ and $W_R{}^-$, heavy neutrino contribution mediated by both $W_L{}^-$ and $W_R{}^-$, triplet Higgs Δ_L contribution mediated by $W_L{}^-$ bosons and RH triplet Higgs Δ_R contribution to NDBD in which the mediator particles are $W_R{}^-$ bosons. The amplitude of these processes are dependent on the mixing between light and heavy neutrinos, the mass of the heavy neutrino, N_i, the mass of the gauge bosons, $W_L{}^-$ and $W_R{}^-$, the elements of the RH leptonic mixing matrix, LH and RH triplet Higgs, Δ_L and Δ_R as well as their coupling to leptons, f_L and f_R. Again, the observation of neutrino oscillation also bestows fascinating evidence for charged lepton flavor violation (CLFV) [54, 55, 56]. Since LFV which is generated at high energy scales are beyond the reach of the colliders, searching them in low energy scales amongst the charged leptons is widely accepted as an alternate procedure to probe LFV at high scales. Many previous works [39, 45, 57, 58]have focussed on the lepton flavor violating decay modes of muon, ($\mu \to 3e$, $\mu \to e\gamma$, $\mu \to e$ conversion in the nuclei). Considerable CLFV occurs in LRSM owing to the contributions that arise from the heavy RH neutrino and Higgs scalars. The relevant branching ratios (BR) has been derived and studied in [54]. The LFV processes $\mu \to 3e$, $\mu \to e\gamma$ provides the most relevant constraints on the masses of the RH neutrinos and the doubly charged scalars. In this work we would consider the process $\mu \to e\gamma$, the BR of which is given by the equation (5.30) as defined in chapter 2 (equation (2.17)),

$$BR\,(\mu \to e\gamma) = 1.5 \times 10^{-7} |g_{lfv}|^2 \left(\frac{1TeV}{M_{W_R}}\right)^4, \tag{5.30}$$

where, g_{lfv} is defined as in equation (2.18). The current experimental constraints for the BRs of these processes has been obtained as $< 1.0 \times 10^{-12}$ for $\mu \to 3e$ at 90% CL was obtained by the SINDRUM experiment. While it is $< 4.2 \times 10^{-13}$ [59] for the process $\mu \to e\gamma$, established by the MEG collaboration.

5.5 Numerical analysis and results

- In LRSM, we can write the light neutrino mass matrix as a combination of type I and type II mass terms as,

$$\mathrm{M}_\nu = \mathrm{M}_\nu{}^{\mathrm{I}} + \mathrm{M}_\nu{}^{\mathrm{II}} \tag{5.31}$$

Here, we consider $\mathrm{M}_\nu{}^{\mathrm{I}}$ to be favoring the TM mixing with magic symmetry, so as to obtain the desired two zero texture. The different magic neutrino mass matrix with two zeroes can be obtained from the most general magic mass matrix which can be parameterized as [27, 28],

$$\mathrm{M}_{\mathrm{magic}} = \begin{bmatrix} p & q & r \\ q & r & p+r-s \\ r & p+r-s & q-r+s \end{bmatrix} \tag{5.32}$$

which can be diagonalized by the TM matrix as,

$\mathrm{M}_{\mathrm{diag}} = \mathrm{U}_{\mathrm{TM2}}{}^{\mathrm{T}}\mathrm{M}_{\mathrm{magic}}\mathrm{U}_{\mathrm{TM2}}$ where, $\mathrm{U}_{\mathrm{TM2}}$ is the diagonalizing matrix for the magic mass matrix and is given in equation (5.3)

- Using the constraint relations for various classes with two zero textures, we can arrive at the mass matrices as,

$$\mathrm{M}_\nu{}^{\mathrm{I}}(\mathrm{A1}) = \begin{bmatrix} 0 & 0 & r \\ 0 & s & r-s \\ r & r-s & -r+s \end{bmatrix}, \mathrm{M}_\nu{}^{\mathrm{I}}(\mathrm{A2}) = \begin{bmatrix} 0 & q & 0 \\ q & s & -s \\ 0 & -s & q+s \end{bmatrix} \tag{5.33}$$

$$\mathrm{M}_\nu{}^{\mathrm{I}}(\mathrm{B1}) = \begin{bmatrix} p & q & 0 \\ q & 0 & p \\ 0 & p & q \end{bmatrix}, \mathrm{M}_\nu{}^{\mathrm{I}}(\mathrm{B2}) = \begin{bmatrix} p & 0 & r \\ 0 & r & p \\ r & p & 0 \end{bmatrix} \tag{5.34}$$

$$\mathrm{M}_\nu{}^{\mathrm{I}}(\mathrm{B3}) = \begin{bmatrix} p & 0 & r \\ 0 & 0 & p+r \\ r & p+r & -r \end{bmatrix}, \mathrm{M}_\nu{}^{\mathrm{I}}(\mathrm{B4}) = \begin{bmatrix} p & q & 0 \\ q & -q & p+q \\ 0 & p+q & 0 \end{bmatrix} \tag{5.35}$$

Again , $M_\nu{}^{I} = U_{TM2}U_{Maj}M_\nu{}^{diag}U_{Maj}{}^{T}U_{TM2}{}^{T}$ where,U_{Maj} consists of the Majorana phases α and β, $M_\nu{}^{diag}$ =diag(m_1, m_2, m_3) which can be written as,

- diag $(m_1, \sqrt{m_1^2 + \Delta m_{sol}^2}, \sqrt{m_1^2 + \Delta m_{sol}^2 + \Delta m_{atm}^2})$ (In NH),
- diag $(\sqrt{m_3^2 + \Delta m_{atm}^2}, \sqrt{m_3^2 + \Delta m_{sol}^2 + \Delta m_{atm}^2}, m_3)$ (In IH),

in terms of the lightest neutrino mass. Thus, by comparing $M_\nu{}^I$ with $M_\nu{}^I$ for different classes we can solve for the unknown parameters (p, q, r, s) in the corresponding matrices and obtain $M_\nu{}^{I}$ for different classes.

- Since now we have $M_\nu{}^{I}$, we can evaluate $M_\nu{}^{II}$ using equation (5.31). Again, we have in LRSM, $M_{RR} = \frac{1}{\gamma}(\frac{M_{W_R}}{M_{W_L}})^2 M_\nu{}^{II}$, where γ is a dimensionless parameter which follows directly from the minimization of the Higgs potential, here we consider its value to be 10^{-10}. Thus we can find out M_{RR} for our further analysis.

- Using the constraint relations for the respective classes, we have compared the neutrino mass matrix, $M_\nu = U_{PMNS}M_\nu{}^{diag}U_{PMNS}{}^{T}$ with the neutrino mass matrices $(M_\nu{}^{I}+M_\nu{}^{II})$ containing two zeros. U_{PMNS} being the diagonalizing matrix of the light neutrino mass matrix, M_ν as defined in equation (1.28). Varying the neutrino parameters, θ_{12}, θ_{13}, δ in its 3σ range [1] and writing the mass eigenvalues in terms of lightest neutrino mass m_1/m_3 for (NH/IH) and varying from 0.0001 to 0.1, we have solved for the parameters α, β and θ_{23}. We have chosen these parameters as the Majorana phases are unknown yet and the precise measurement of θ_{23} and octant degeneracy is yet to be determined although experiments like NOvA, T2K have reported some values.

- The different structures of the neutrino mass matrix in the LRSM using two texture zero are shown in table 5.8. The symmetry realizations of the texture zeros using the cyclic groups $Z8 \times Z2$ are as shown in the previous section .

- Owing to the presence of new scalars and gauge bosons in the LRSM, various additional sources would give rise to contributions to NDBD process, which involves RH neutrinos, RH gauge bosons, scalar Higgs triplets as well as the mixed LH-RH contributions. We will study LNV (NDBD) for the non-standard contributions for the effective mass in the framework of LRSM. For a simplified analysis, we would ignore the left-right gauge boson mixing $(W_L - W_R)$ which is very less and heavy light neu-

Class	M_D	M_{RR}	$M_\nu{}^I$	$M_\nu{}^{II}$	M_ν
A1	$\begin{bmatrix} x & 0 & 0 \\ 0 & y & 0 \\ 0 & 0 & z \end{bmatrix}$	$\begin{bmatrix} A & B & C \\ B & D & 0 \\ C & 0 & 0 \end{bmatrix}$	$\begin{bmatrix} 0 & 0 & a \\ 0 & b & c \\ a & c & d \end{bmatrix}$	$\begin{bmatrix} 0 & 0 & W \\ 0 & X & Y \\ W & Y & Z \end{bmatrix}$	$\begin{bmatrix} 0 & 0 & W+a \\ 0 & X+b & Y+c \\ W+a & Y+c & Z+d \end{bmatrix}$
A2	$\begin{bmatrix} x & 0 & 0 \\ 0 & y & 0 \\ 0 & 0 & z \end{bmatrix}$	$\begin{bmatrix} A & B & C \\ B & 0 & 0 \\ C & 0 & D \end{bmatrix}$	$\begin{bmatrix} 0 & a & 0 \\ a & b & c \\ 0 & c & d \end{bmatrix}$	$\begin{bmatrix} 0 & W & 0 \\ W & X & Y \\ 0 & Y & Z \end{bmatrix}$	$\begin{bmatrix} 0 & W+a & 0 \\ W+a & X+b & Y+c \\ 0 & Y+c & Z+d \end{bmatrix}$
B1	$\begin{bmatrix} x & 0 & 0 \\ 0 & y & 0 \\ 0 & 0 & z \end{bmatrix}$	$\begin{bmatrix} A & B & C \\ B & D & E \\ C & E & F \end{bmatrix}$	$\begin{bmatrix} a & b & 0 \\ b & 0 & c \\ 0 & c & d \end{bmatrix}$	$\begin{bmatrix} W & X & 0 \\ X & 0 & Y \\ 0 & Y & Z \end{bmatrix}$	$\begin{bmatrix} W+a & X+b & 0 \\ X+b & 0 & Y+c \\ 0 & Y+c & Z+d \end{bmatrix}$
B2	$\begin{bmatrix} x & 0 & 0 \\ 0 & y & 0 \\ 0 & 0 & z \end{bmatrix}$	$\begin{bmatrix} A & B & C \\ B & D & E \\ C & E & F \end{bmatrix}$	$\begin{bmatrix} a & 0 & b \\ 0 & c & d \\ b & d & 0 \end{bmatrix}$	$\begin{bmatrix} W & 0 & X \\ 0 & Y & Z \\ X & Z & 0 \end{bmatrix}$	$\begin{bmatrix} W+a & 0 & X+b \\ 0 & Y+c & Z+d \\ X+b & Z+d & 0 \end{bmatrix}$
B3	$\begin{bmatrix} x & 0 & 0 \\ 0 & y & 0 \\ 0 & 0 & z \end{bmatrix}$	$\begin{bmatrix} A & B & 0 \\ B & C & D \\ 0 & D & 0 \end{bmatrix}$	$\begin{bmatrix} a & 0 & b \\ 0 & 0 & c \\ b & c & d \end{bmatrix}$	$\begin{bmatrix} W & 0 & X \\ 0 & 0 & Y \\ X & Y & Z \end{bmatrix}$	$\begin{bmatrix} W+a & 0 & X+b \\ 0 & 0 & Y+c \\ X+b & Y+c & Z+d \end{bmatrix}$
B4	$\begin{bmatrix} x & 0 & 0 \\ 0 & y & 0 \\ 0 & 0 & z \end{bmatrix}$	$\begin{bmatrix} A & 0 & B \\ 0 & 0 & C \\ B & C & D \end{bmatrix}$	$\begin{bmatrix} a & b & 0 \\ b & c & d \\ 0 & d & 0 \end{bmatrix}$	$\begin{bmatrix} W & X & 0 \\ X & Y & Z \\ 0 & Z & 0 \end{bmatrix}$	$\begin{bmatrix} W+a & X+b & 0 \\ X+b & Y+c & Z+d \\ 0 & Z+d & 0 \end{bmatrix}$

Table 5.8: The structures of M_D, M_{RR}, $M_\nu{}^I$ and $M_\nu{}^{II}$ and M_ν for different classes of two zero textures.

trino mixing which is dependent upon $\frac{M_D}{M_R}$ is $\zeta \approx 10^{-6}$. Furthermore, contributions from the LH contributions to $0\nu\beta\beta$ can be neglected. The total effective mass is thus given by the formula (5.36) as used in earlier works like [42] for classes A1 and A2.

$$m_{N+\Delta}{}^{eff} = p^2 \frac{{M_{W_L}}^4}{{M_{W_R}}^4} \frac{{U_{Rei}}^* 2}{M_i} + p^2 \frac{{M_{W_L}}^4}{{M_{W_R}}^4} {U_{Rei}}^2 M_i \left(\frac{1}{{M_{\Delta_R}}^2} + \frac{1}{{M_{\Delta_R}{}'}^2} + \frac{1}{{M_{\Delta_R}{}''}^2} + \frac{1}{{M_{\Delta_R}{}'''}^2} \right). \tag{5.36}$$

and it is,

$$m_{N+\Delta}{}^{eff} = p^2 \frac{{M_{W_L}}^4}{{M_{W_R}}^4} \frac{{U_{Rei}}^* 2}{M_i} + p^2 \frac{{M_{W_L}}^4}{{M_{W_R}}^4} {U_{Rei}}^2 M_i \left(\frac{1}{{M_{\Delta_R}}^2} + \frac{1}{{M_{\Delta_R}{}'}^2} + \frac{1}{{M_{\Delta_R}{}''}^2} \right). \tag{5.37}$$

for the classes B1 to B4. Here, Δ in LHS represents the RH scalar triplets, $< p^2 >= m_e m_p \frac{M_N}{M_\nu}$ is the typical momentum exchange of the process, where m_p and m_e are the mass of the proton and electron respectively and M_N is the NME corresponding to the RH neutrino exchange. U_{Rei} in equations (5.36) and (5.37) denotes the elements of the first row of the unitary matrix diagonalizing the RH neutrino mass matrix M_{RR} with mass eigenvalues M_i. Since we have M_{RR}, we can evaluate U_{Rei} by diagonalizing it as, $M_{RR} = U_R {M_{RR}}^{diag} {U_R}^T$. The M_{RR} we obtain would consist of the mixing angles in the TM mass matrix, θ and ϕ along with the other parameters of our concern. As shown in paper [27, 26], θ and ϕ are related to the oscillation parameters θ_{23} and θ_{12} as,

$$\mathrm{Sin}{\theta_{12}}^2 = \frac{1}{3 - 2\mathrm{Sin}^2\theta}, \mathrm{Sin}{\theta_{23}}^2 = \frac{1}{2}(1 + \frac{\sqrt{3}\mathrm{Sin}2\theta\mathrm{Cos}\phi}{3 - 2\mathrm{Sin}^2\theta}) \tag{5.38}$$

We thus obtained the parameter space for θ and ϕ by varying the parameters θ_{12} and θ_{23} in its 3 σ range which is shown in figure 5.1. We have seen that the trimaximal mixing angle θ lies within the range (0.05 to 0.5) radian for the 3σ range of the solar mixing angle θ_{12} although it doesn't show significant dependence. The other mixing angle ϕ shows some dependence on the atmospheric mixing angle θ_{23} for both normal and inverted ordering of neutrino mass. It's values lies within (1.56-1.66) radian for the 3σ range of θ_{23}. The plot shows an exponential decrease and then increase in ϕ with the increase in θ_{23} with a fall at around the best fit value.

The effective mass governing NDBD from the new physics contribution coming from RH neutrino and scalar triplet can be obtained from equations (5.36) and (5.37). We have shown the two-parameter contour plots with effective Majorana mass as the contour as in figures 5.2 to 5.19. In figures 5.2 to 5.7, we have shown the two-parameter space for $m_{lightest}$ Vs ϕ, θ Vs β and α Vs β for both the mass hierarchies for different classes of allowed two texture zero neutrino mass. The KamLAND-Zen upper limit for the effective mass is shown in the contour.

- In figure 5.2 and 5.3, it is seen that the value of lightest neutrino mass ranging from (0.01 to 0.1) eV satisfies the KamLAND-Zen limit of effective mass in all the classes irrespective of the mass hierarchies. Whereas, the TM mixing angle ϕ for all the classes shows different results. In NH, for the classes A1, B1 and B4, the range of ϕ satisfying the experimental bound of effective mass lies from around (1.57-1.60) radian and for the classes A2, B2 and B3, it is around (1.62-1.66) radian. For IH again the classes A1, B1, B2 and B4 has ϕ around (1.57-1.6) radian whereas A2 and B3 has the range (1.62-1.66) for ϕ satisfying KamlAND-Zen limit.

- In figure 5.4 and 5.5, i.e., β Vs θ plot, it is seen that for NH, the classes A1, A2, B1, B2, B3 has θ ranging from (0.05-0.35) radian whereas B4 has θ from (0.45-0.55) radian which satisfies the experimental bounds of effective neutrino mass. For IH, A1, A2, B1, B2 and B3 has θ from (0.05-0.3) radian whereas B4 has the range (0.45-0.55) radian. Similarly, the value of the Majorana phase β is also constrained as seen from these

plots. It is around (1-3) radian for classes A1, A2, B1, B2 and B3 for NH and (0.8-3) radian for the class B4 which satisfies the KamLAND-Zen bound. For IH again, A1, A2, B1, B2 and B3 have range around (1-3.2) radian, whereas it is around (0.6-3.2) radian for B4.

- In figure 5.6 and 5.7, again we see that the value of the Majorana phase α is also constrained for the experimentally allowed range of effective mass. It is different for the different classes of allowed two zero texture neutrino mass. We have summarized the range of the parameters satisfying the experimental bound of effective neutrino mass governing NDBD in table 5.9 and 5.10

- Figures 5.8 to 5.19 shows the two-parameter contour plots with the new physics contribution to effective mass as the contour, where (0.061-0.1) eV is the KamLAND-Zen upper limit for effective neutrino mass governing NDBD. The parameters shown being the model parameters that appear in the type II SS mass matrix as shown in table 5.8. Since there are four parameters, W, X, Y, Z in the type II SS mass matrix, there would be ${}^4C_2$, i.e., 6 combinations of two parameters for all the classes which we have shown in these plots. The figures correspond to normal and inverted hierarchies which we have shown using different contours to distinguish them. The values of these parameters which gives effective mass within experimental bounds are summarized in table 5.11. Although all the classes (A1, A2, B1, B2, B3, B4) gives the allowed values of effective mass, in some cases the values are so much constrained like A2 (IH), B1 (IH), B2 (NH).

- For lepton flavor violation, we have evaluated the BR for the process $\mu \to e\gamma$ using equation (5.30), where V is the mixing matrix of the RH neutrinos with the electrons and muons. $\mathrm{M_n}(\mathrm{n} = 1, 2, 3)$ are the RH neutrino masses. It is evident from the equation for the BR that it is dependent upon $[M_R M_R{}^*]_{\mu e}$. We evaluated the BR and have shown the variation with the Majorana phase β and atmospheric mixing angle θ_{23}. Figure (5.20) and (5.21) shows the contour plot with BR for the decay process $(\mu \to e\gamma)$ as the contour where 4.2×10^{-13} is the upper limit of BR as given by MEG experiment. It is interestingly seen that most of the classes are unable to explain the LFV as far as experimental bounds are concerned. Thus only the class B3 is satisfying

the experimental bound of BR for both the hierarchies. On careful observation of the figure, we see that for the 3σ range of θ_{23}, the value of the Majorana phase, β is constrained to 1 to 3 radian.

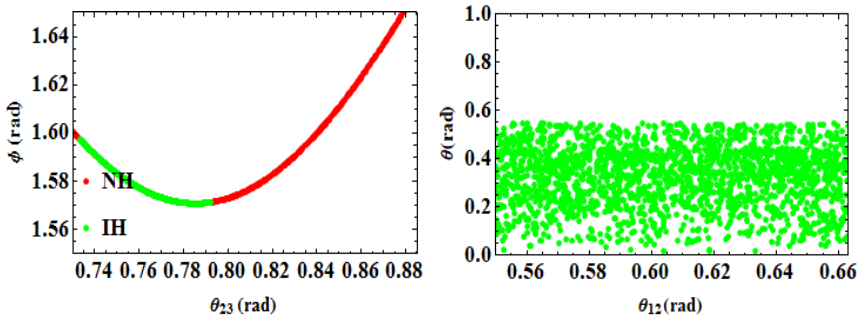

Figure 5.1: Variation of the TM mixing angle ϕ and θ with the atmospheric and solar mixing angle, θ_{23} and θ_{12}.

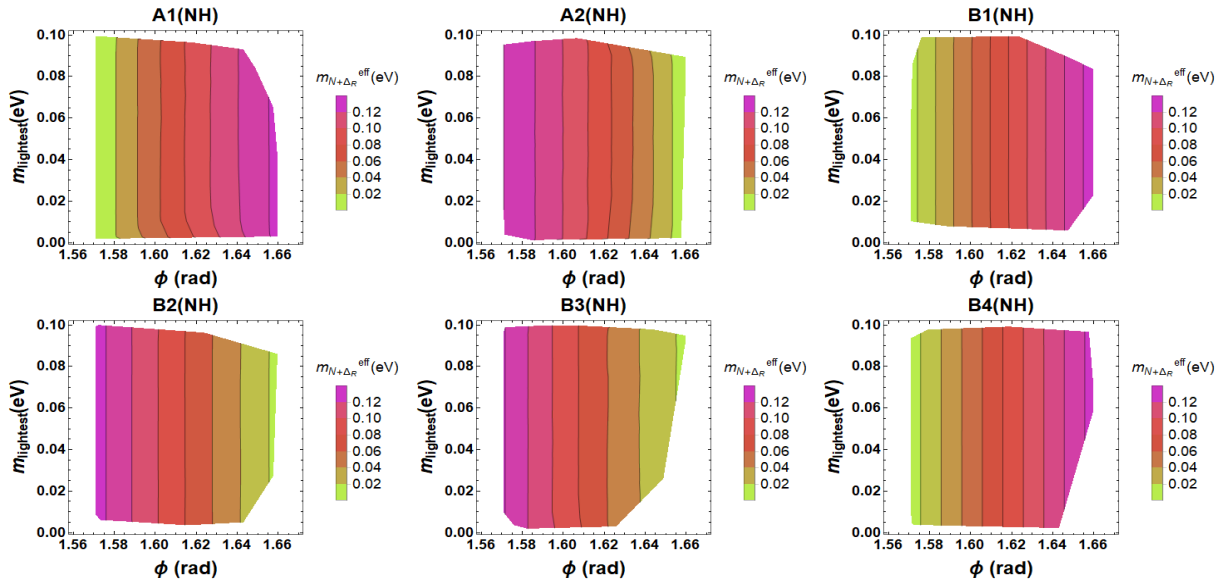

Figure 5.2: New physics contribution to effective mass governing NDBD for different classes of 2-0 textures for NH shown as a function of two parameter $m_{lightest}$ and ϕ. The contour represents the eff. mass where 0.061 eV is the KamLAND-Zen upper limit.

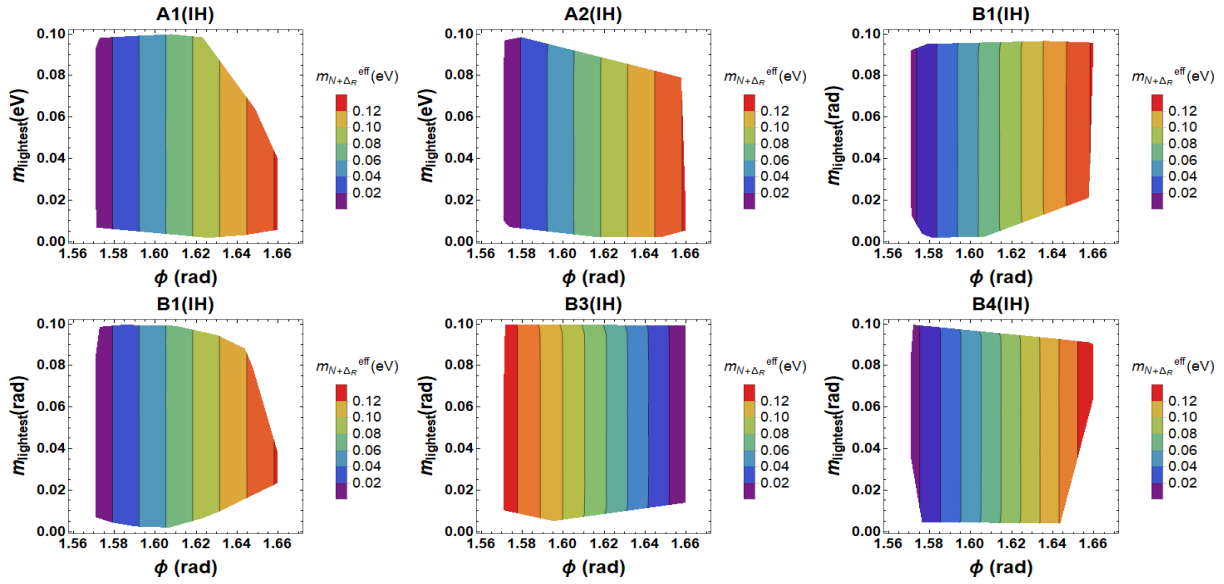

Figure 5.3: New physics contribution to effective mass governing NDBD for different classes of 2-0 textures for IH shown as a function of two parameter $m_{lightest}$ and ϕ. The contour represents the eff. mass where 0.061 eV is the KamLAND-Zen upper limit.

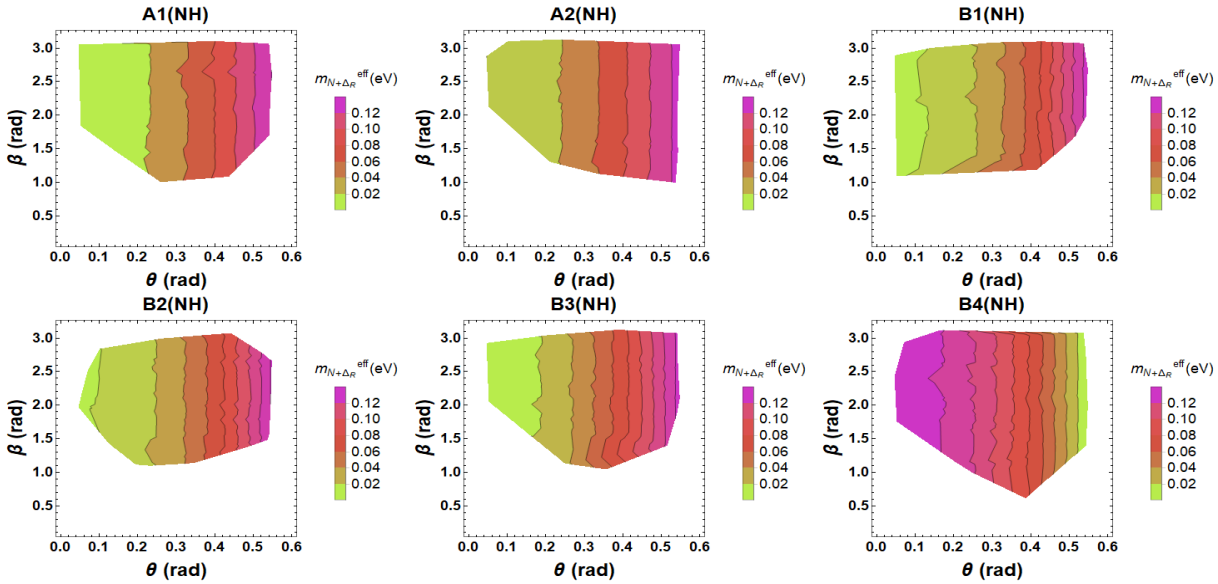

Figure 5.4: New physics contribution to effective mass governing NDBD for different classes of 2-0 textures for IH shown as a function of two parameter θ and β. The contour represents the eff. mass where 0.061 eV is the KamLAND-Zen upper limit.

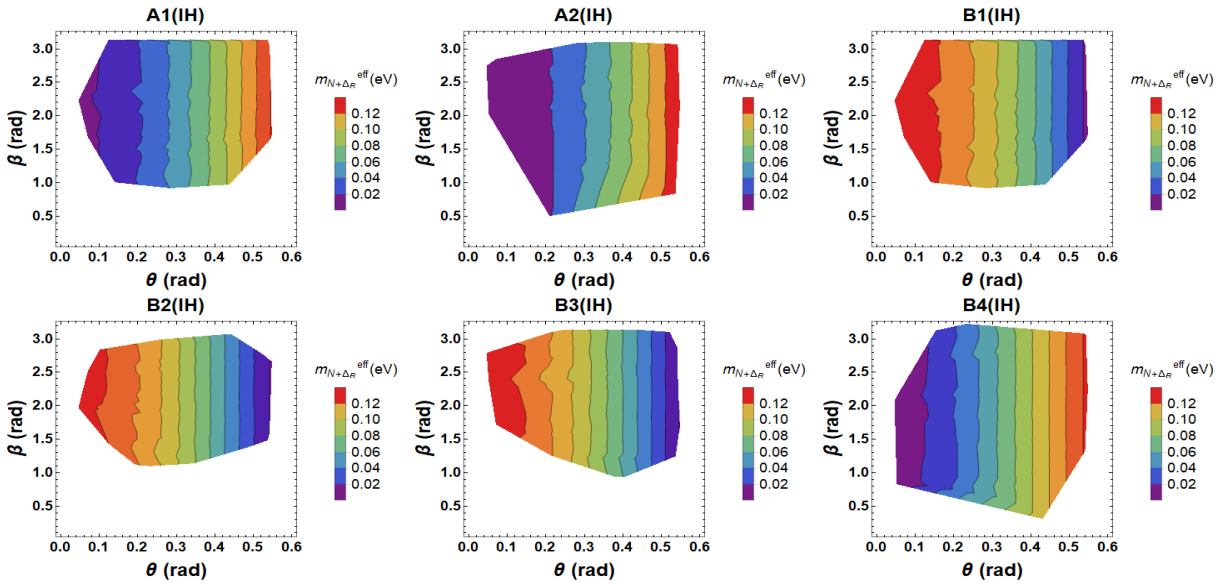

Figure 5.5: New physics contribution to effective mass governing NDBD for different classes of 2-0 textures for IH shown as a function of two parameter θ and β. The contour represents the eff. mass where 0.061 eV is the KamLAND-Zen upper limit.

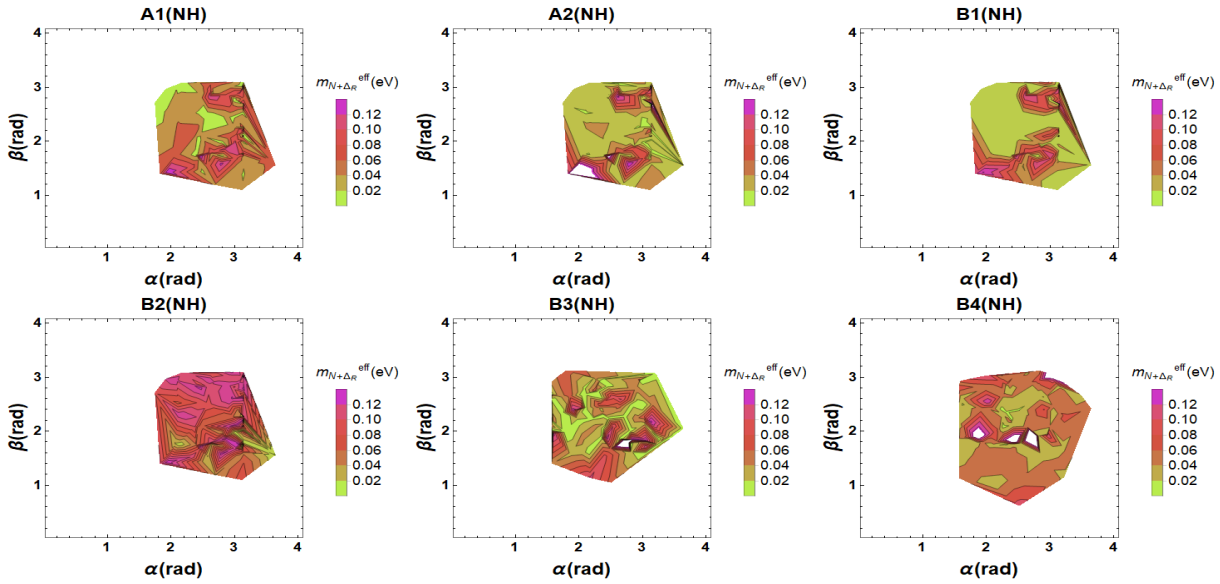

Figure 5.6: New physics contribution to effective mass governing NDBD for different classes of 2-0 textures for IH shown as a function of two parameter α and β. The contour represents the eff. mass where 0.061 eV is the KamLAND-Zen upper limit.

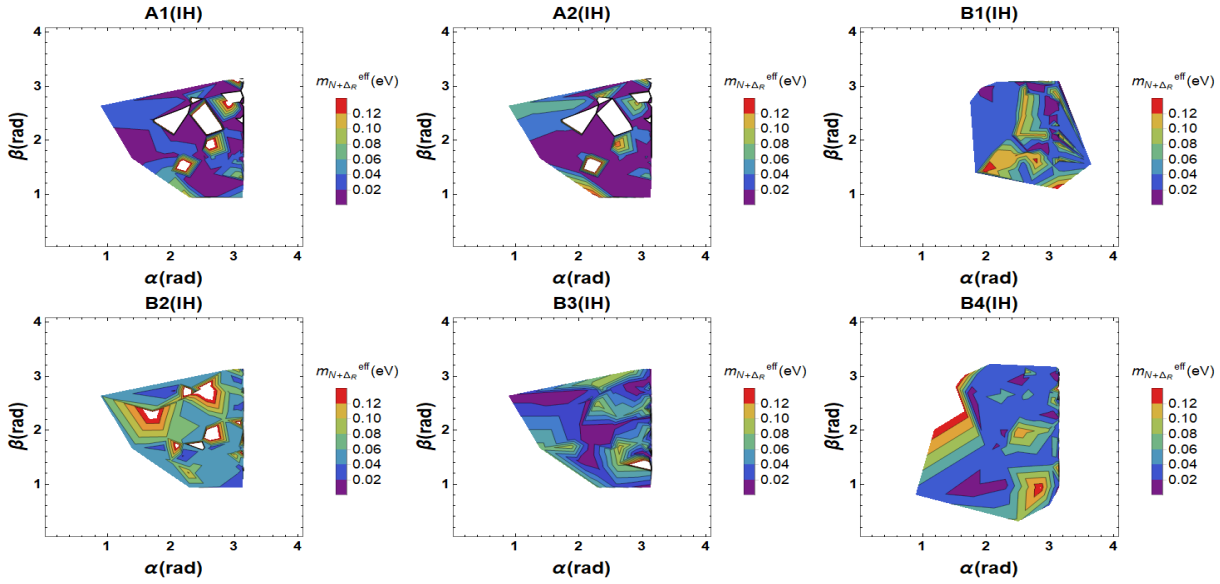

Figure 5.7: New physics contribution to effective mass governing NDBD for different classes of 2-0 textures for IH shown as a function of two parameter α and β. The contour represents the eff. mass where 0.061 eV is the KamLAND-Zen upper limit.

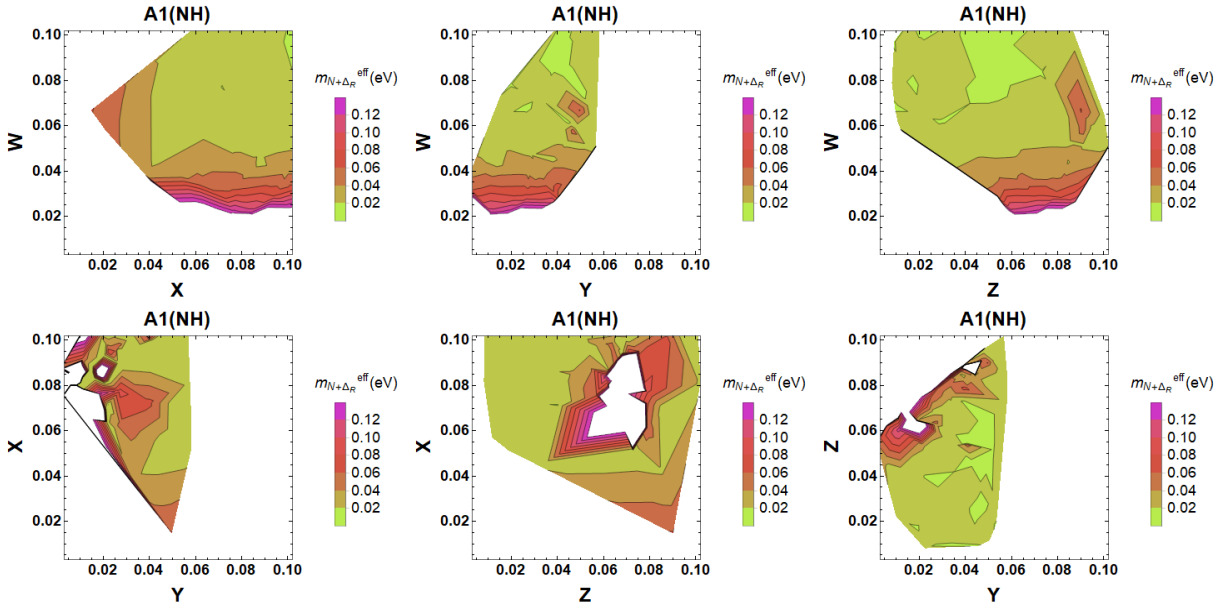

Figure 5.8: The various combinations of type II SS model parameters (in eV) with the effective mass as the contour for A1 (NH).

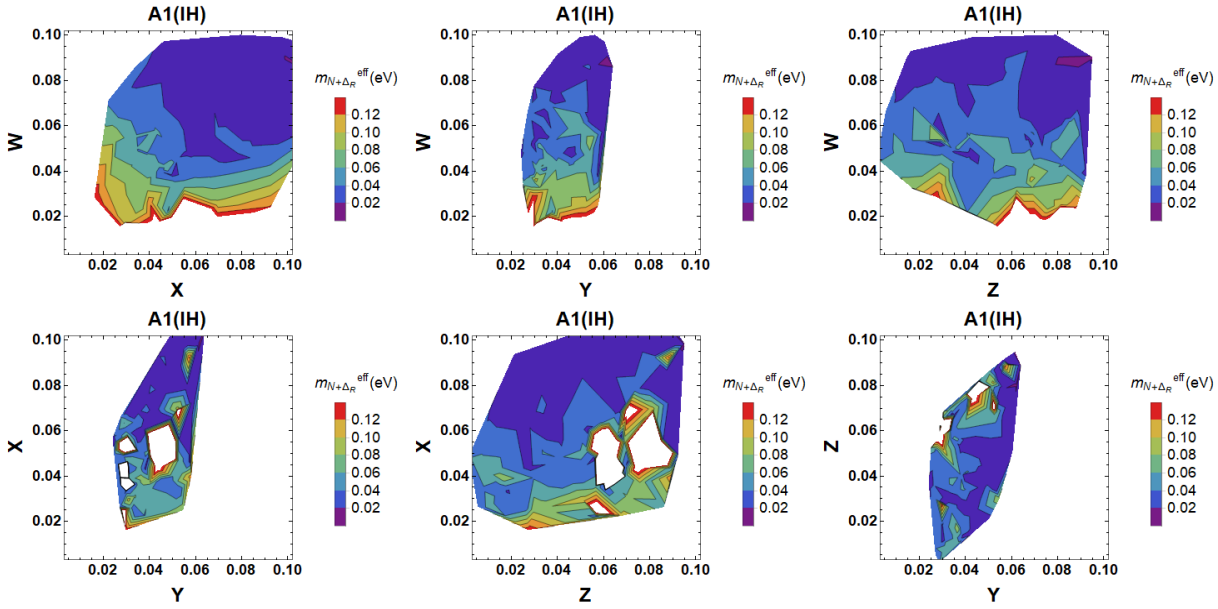

Figure 5.9: The various combinations of type II SS model parameters (in eV) with the effective mass as the contour for A1 (IH).

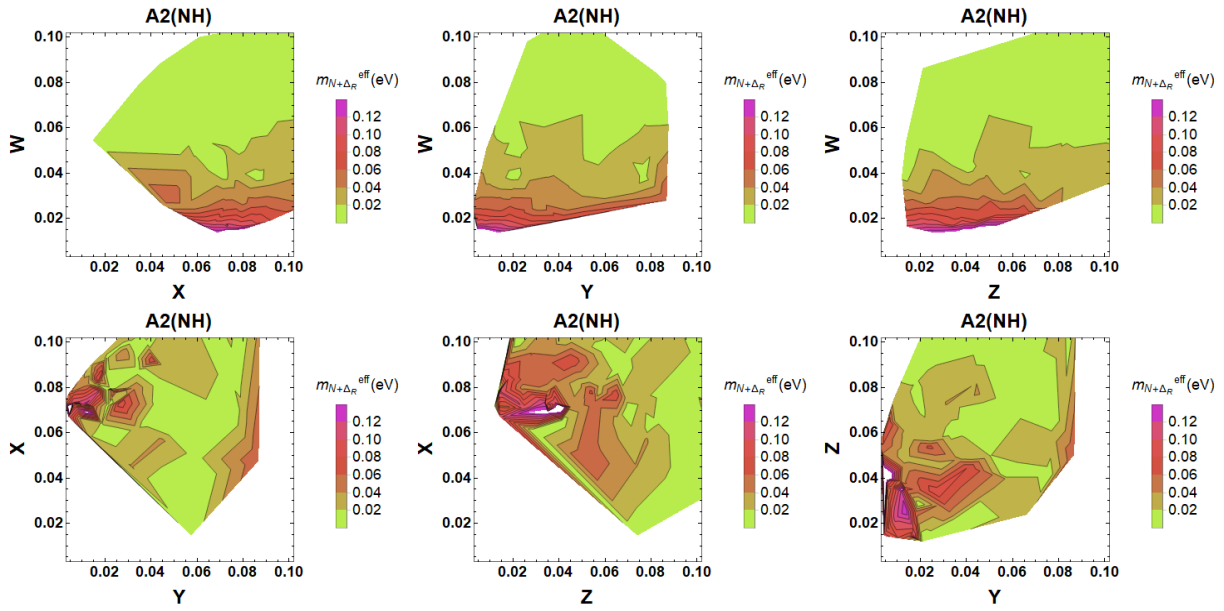

Figure 5.10: The various combinations of type II SS model parameters (in eV) with the effective mass as the contour for A2 (NH).

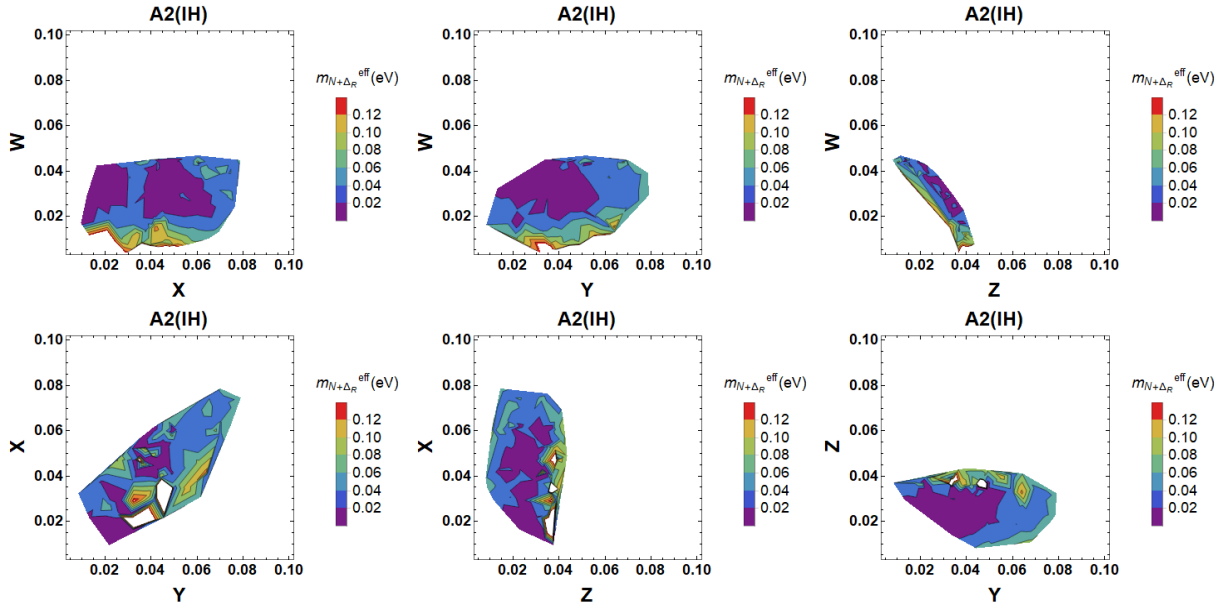

Figure 5.11: The various combinations of type II SS model parameters (in eV) with the effective mass as the contour for A2 (IH).

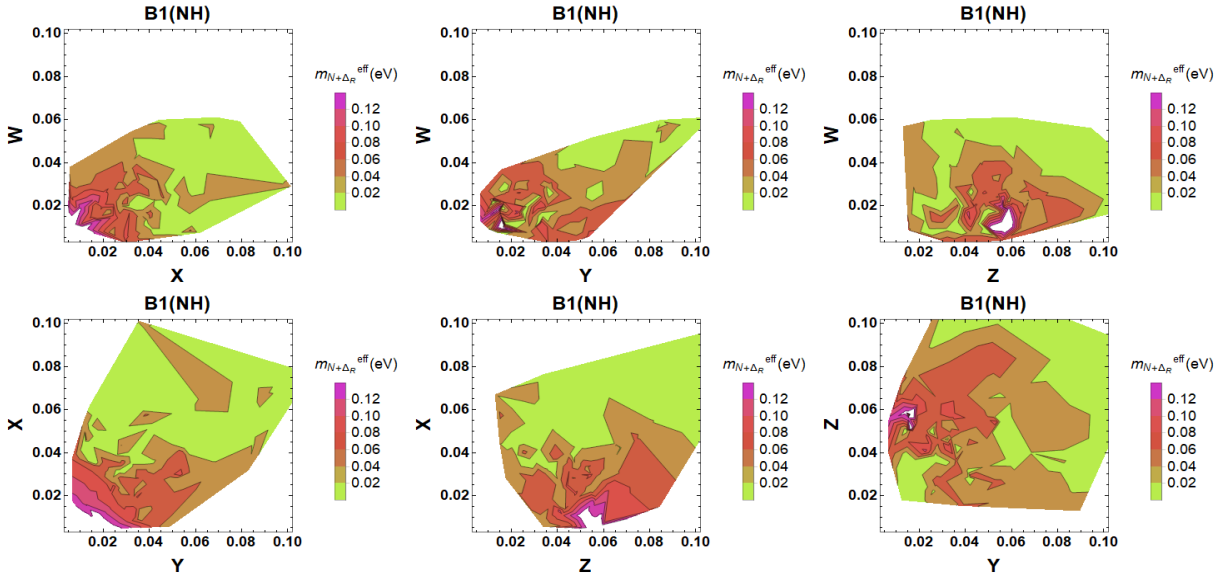

Figure 5.12: The various combinations of type II SS model parameters (in eV) with the effective mass as the contour for B1 (NH).

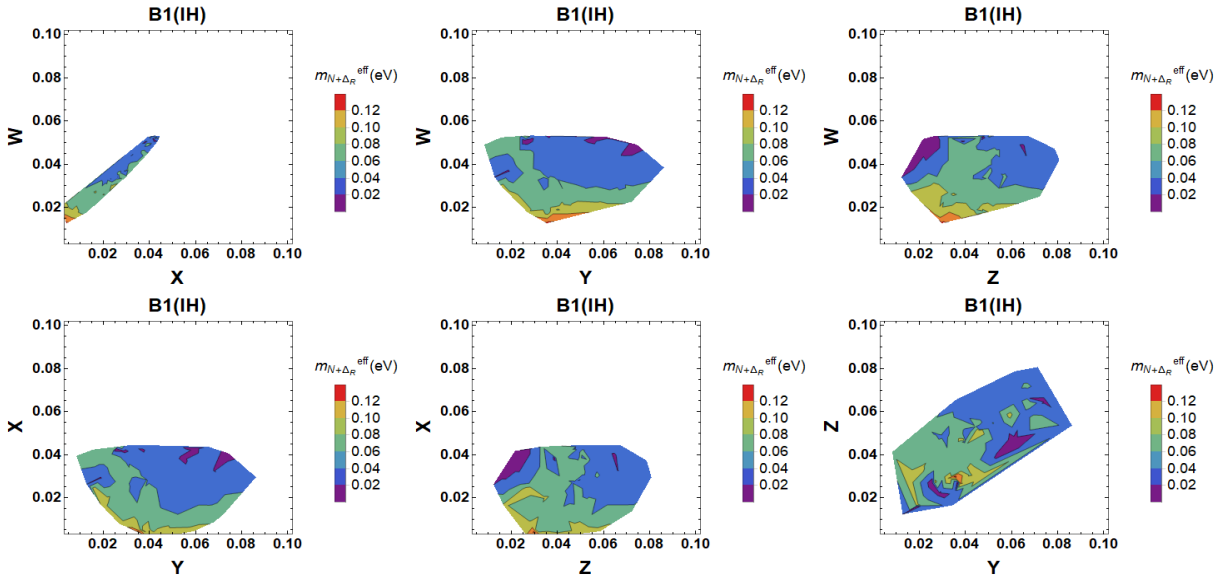

Figure 5.13: The various combinations of type II SS model parameters (in eV) with the effective mass as the contour for B1 (IH).

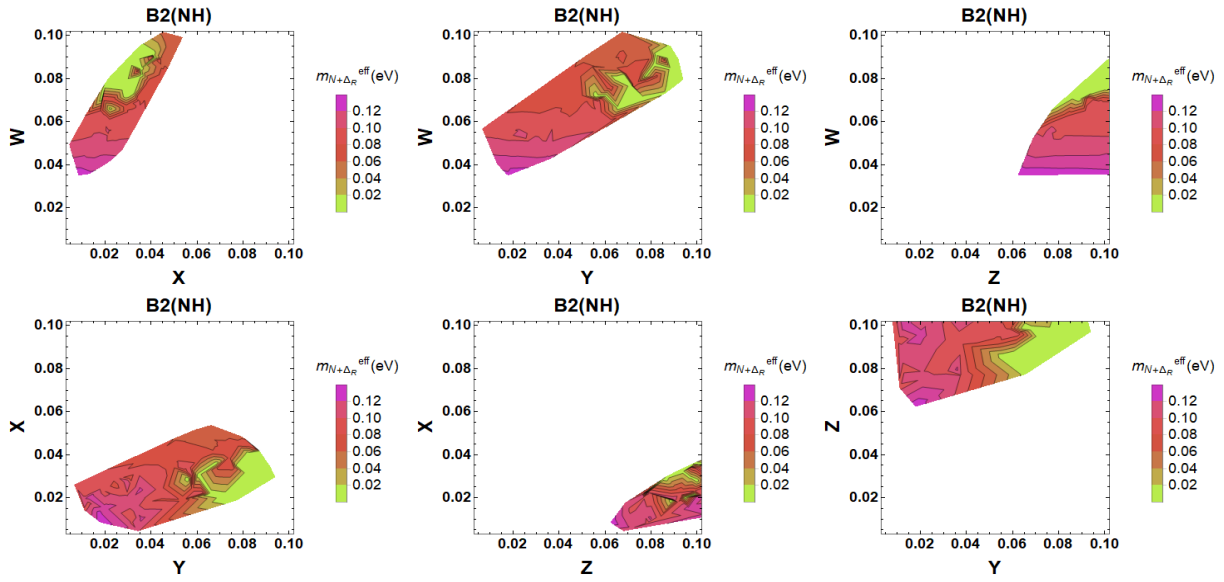

Figure 5.14: The various combinations of type II SS model parameters (in eV) with the effective mass as the contour for B2 (NH).

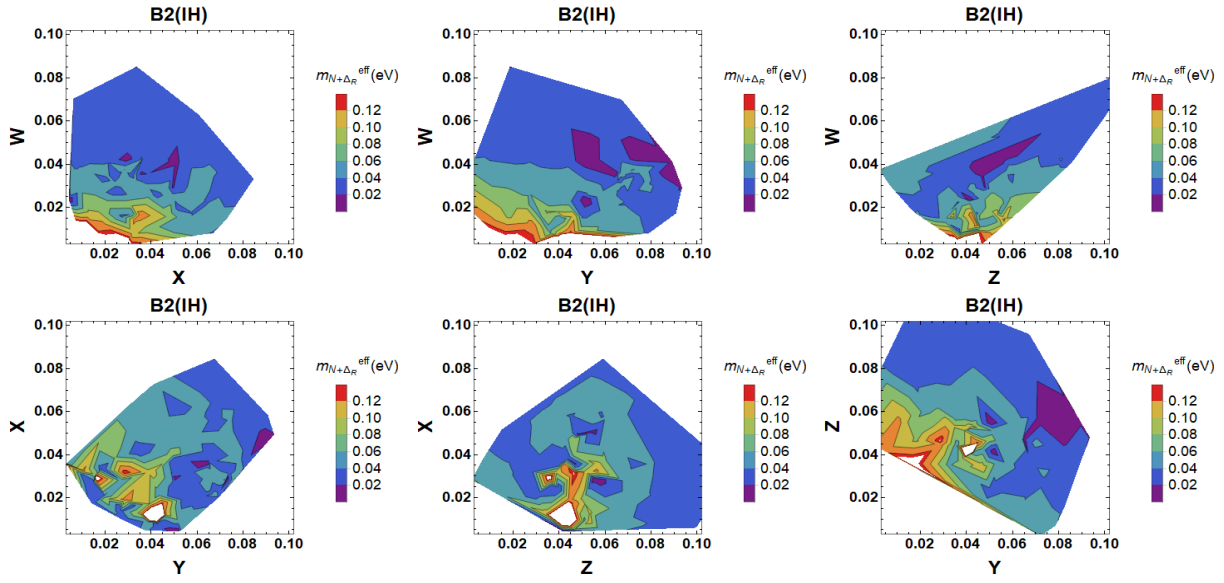

Figure 5.15: The various combinations of type II SS model parameters (in eV) with the effective mass as the contour for B2 (IH).

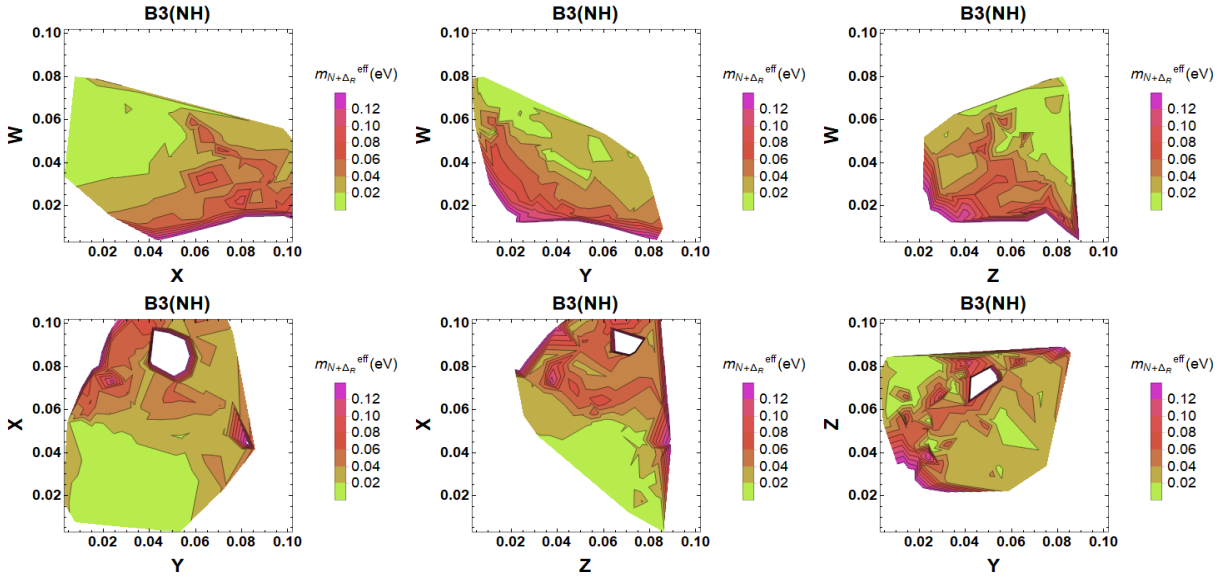

Figure 5.16: The various combinations of type II SS model parameters (in eV) with the effective mass as the contour for B3 (NH).

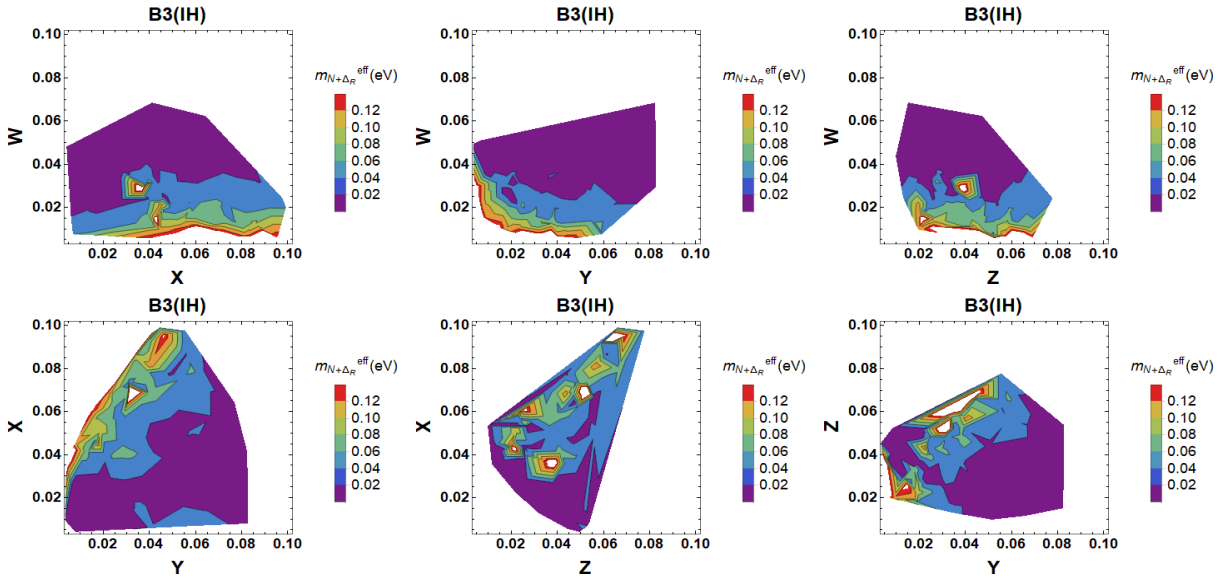

Figure 5.17: The various combinations of type II SS model parameters (in eV) with the effective mass as the contour for B3 (IH).

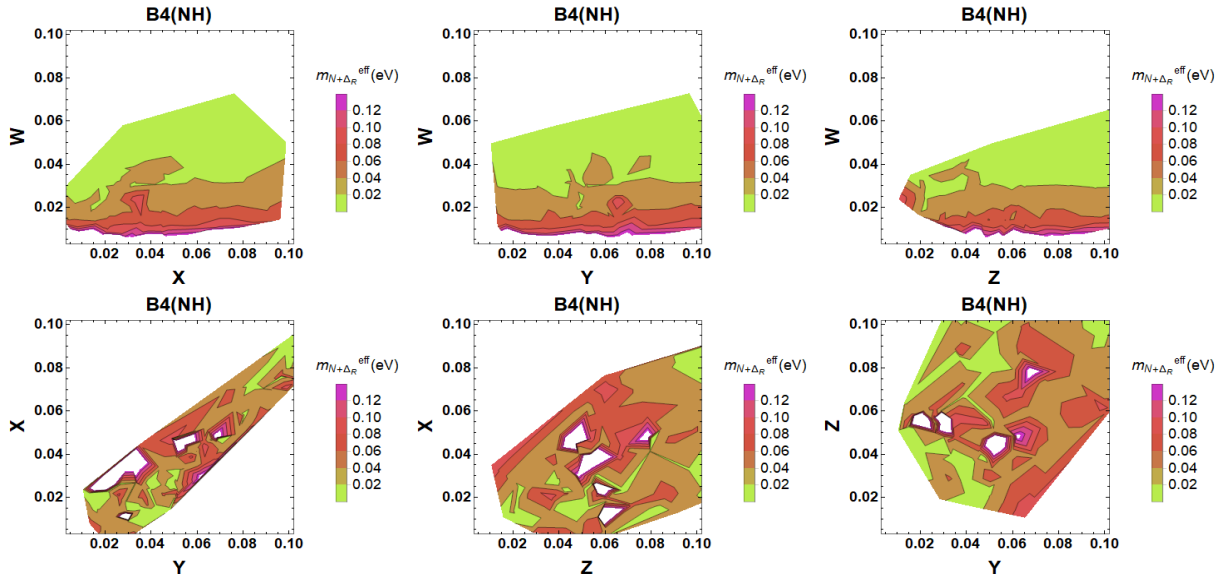

Figure 5.18: The various combinations of type II SS model parameters (in eV) with the effective mass as the contour for B4 (NH).

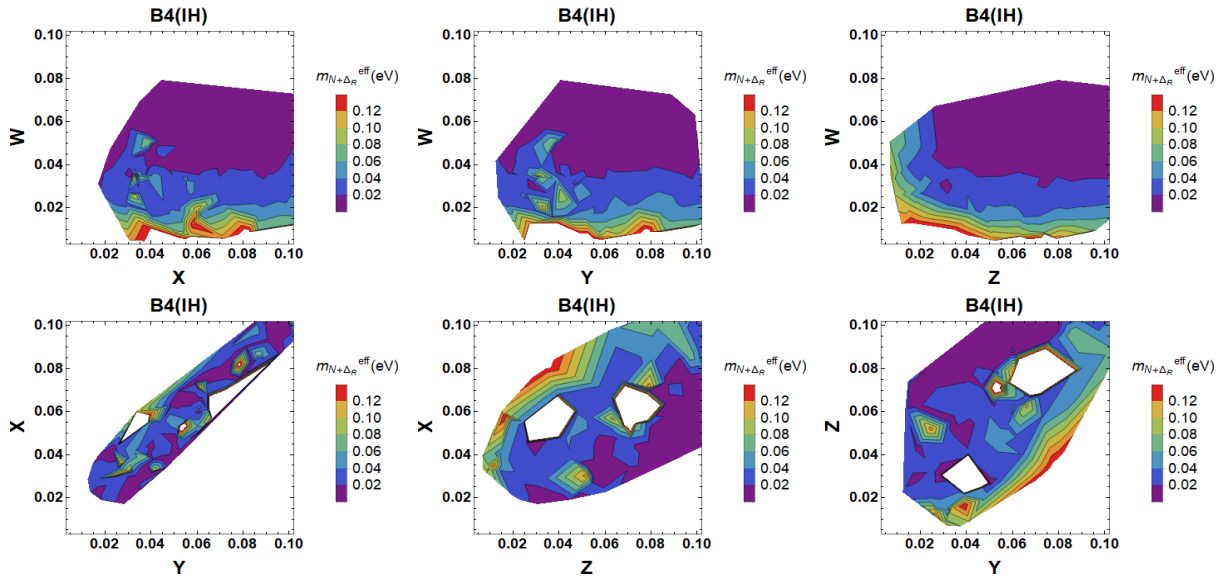

Figure 5.19: The various combinations of type II SS model parameters (in eV) with the effective mass as the contour for B4 (IH).

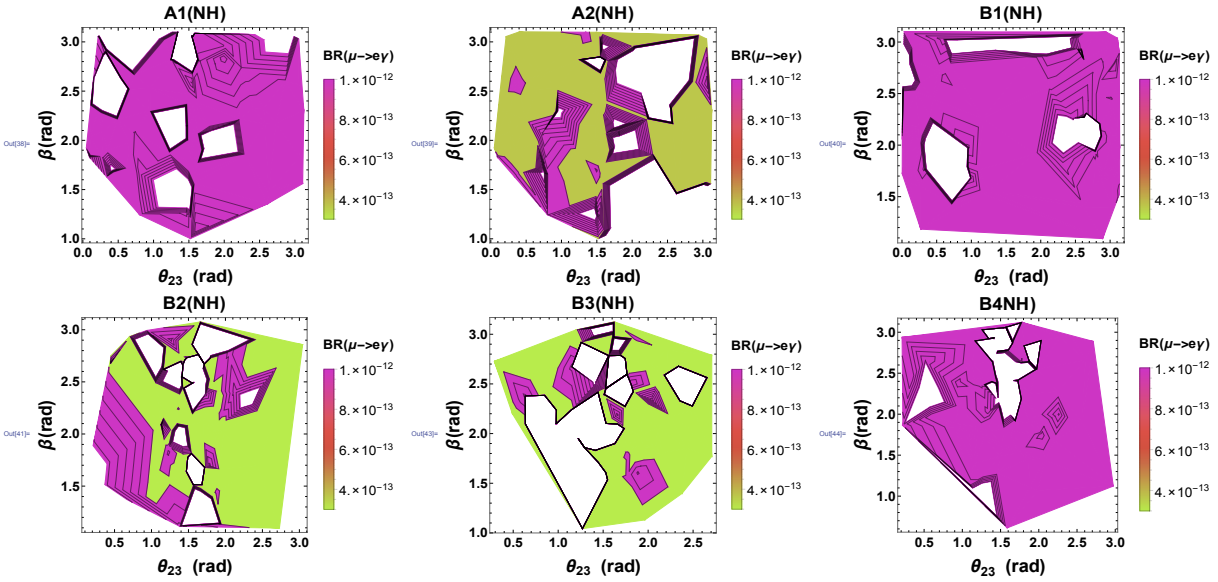

Figure 5.20: Atmospheric mixing angle, θ_{23} Vs Majorana phase α (for NH) with BR for $\mu \to e\gamma$ as the contour where 4.2×10^{-13} is the upperlimit for BR given by MEG experiment.

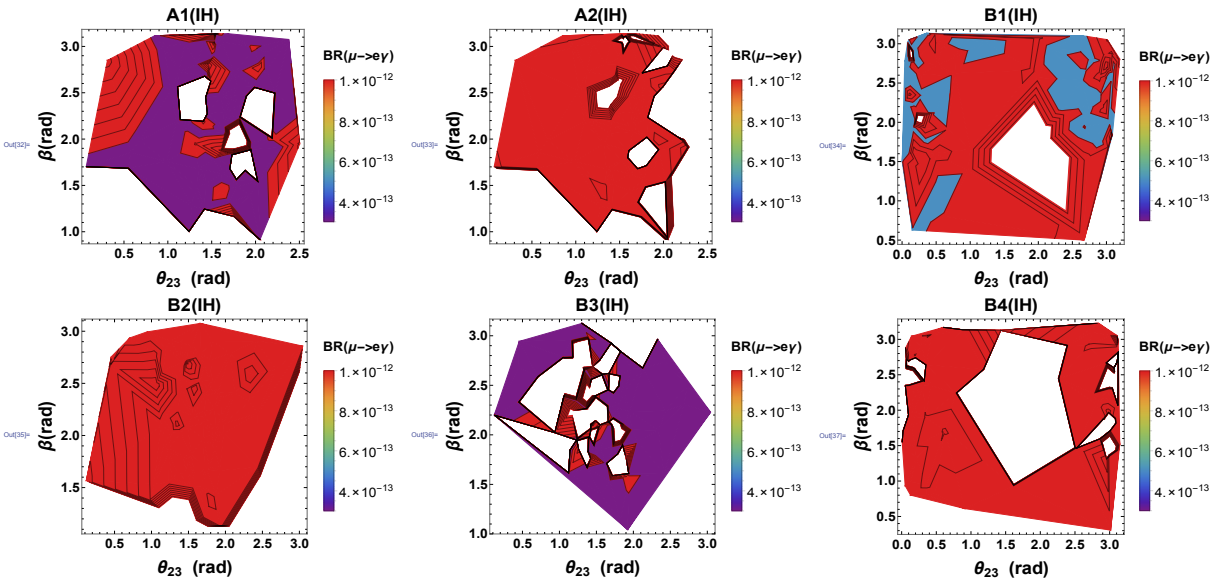

Figure 5.21: Atmospheric mixing angle, θ_{23} Vs Majorana phase α (for IH) with BR for $\mu \to e\gamma$ as the contour where 4.2×10^{-13} is the upper limit for BR given by MEG experiment.

5.5.1 Collider signatures

Physics at the TeV scale has obtained great importance owing to the fact that it can be probed at the colliders. Characteristic signatures of the LRSM (which is the framework of

our concern) at the hadron collider experiments like LHC emerges from the production and decay of triply and doubly charged scalars of the scalar quadruplet. In TeV scale LRSM, the presence of RH gauge interactions as well as the mixing between the heavy and light neutrinos lead via the production of the RH gauge boson, W_R to significant signal strength for the $l^{\pm}l^{\pm}jj$ channel. In the colliders, W_R could be produced through Drell-Yan, which decays to RH neutrino and a charged lepton. The RH neutrino (which are Majorana particles) can further decay to charged leptons/antileptons and jets. With negligible mixing between heavy and light neutrinos as well as left and right W bosons, both W_R and N_R couple through RH currents. Several constraints have been put forwarded on the mass of the RH gauge boson, W_R, the breaking scale of LRSM based on low energy processes like leptogenesis, supersymmetry, neutrinoless double beta decay etc. Most stringent experimental constraints on the masses of W_R, M_N in MLRSM as explained in [60] are provided by $l^{\pm}l^{\pm}jj$ searches in ATLAS, dijet searches by ATLAS (CMS), neutral hadron transitions and search for NDBD. When the breaking scale of LRSM is low enough, LNV can be seen and hence the Majorana nature of the neutrino mass can be probed in the colliders and in future experiments in a wider range of parameter space. Since we are considering the low energy phenomena like NDBD and LFV, we are considering the experimental bounds on these mass provided by the search for these phenomenon. The NDBD experiments are mainly focused on determining the effective Majorana neutrino mass $< m_{\beta\beta} >$ which is related to the observed NDBD lifetime as,

$$\frac{1}{T_{\frac{1}{2}}{}^{0\nu}} = G^{0\nu}(Q,Z)\left|M^{0\nu}\right|^2 \frac{\left|m_{\beta\beta}\right|^2}{{m_e}^2}, \tag{5.39}$$

where the terms $G_{0\nu}$, M_ν and m_e represents the phase space factor, the nuclear matrix element (NME) and the electron mass respectively. Γ represents the decay width for $0\nu\beta\beta$ decay process. The best lower limits on the NDBD half-life has been obtained for the isotopes Ge-76, Te-130, Xe-136 in notable experiments like GERDA-II, CUORE, KamLAND-Zen respectively. The non-observation of NDBD constraints the masses of W_R and N_R as, $\sum_i \frac{{Y_{ei}}^2}{M_i {M_{W_R}}^4} \leq (0.082\text{-}0.076)\ TeV^{-5}$ using 90% CL from the limit propounded by KamLAND-Zen $T^{0\nu}_{1/2} > 1.07 \times 10^{26}$ which corresponds to an effective mass of $| < m_{eff} > | < (0.061 - 0.065)eV$ [61] where the range corresponds to the uncertainities in the NMEs of the relevant process. For M_{W_R} of 3 (5 TeV), the mass of the RH $\nu \geq$ 150-162 GeV (19.5-21)GeV. Again, Tello et al. [62] found the lower bound on mass of ${\Delta_R}^{++}$ to be,

$$M_{\Delta_R}^{++} \geq 500 \left(\frac{3.5TeV}{M_{W_R}}\right)^2 \times \sqrt{\frac{M_N}{3TeV}}. \tag{5.40}$$

Considering these experimental bounds in mind, we have considered the mass of W_R as 3.5 TeV in accordance with the collider probes and the other heavy particles of the order of TeV.

Class	$\alpha(rad)$ (NH/IH)	$\beta(rad)$(NH/IH)	$m_{lightest}(eV)$(NH/IH)
A1	1.8-3.8/1.0-3.2	1.0-3.0/1.0-3.2	0.01-0.1/0.01-0.1
A2	1.8-3.8/1.0-3.2	1.0-3.0/1.0-3.2	0.01-0.1/0.01-0.1
B1	1.8-3.8/1.8-3.6	1.0-3.0/1.2-3.2	0.01-0.1/0.01-0.1
B2	2.0-3.6/1.5-3.2	1.2-3.0/1.0-2.8	0.01-0.1/0.01-0.1
B3	1.8-3.6/1.0-3.2	1.2-3.0/1.0-3.0	0.01-0.1/0.01-0.1
B4	1.6-3.6/0.9-3.2	0.8-3.0/0.6-3.2	0.01-0.1/0.01-0.1

Table 5.9: The range of parameters (α, β and $m_{lightest}$) that satisfies the KamLAND-Zen limit of effective Majorana neutrino mass.

Class	$\theta(rad)$ (NH/IH)	$\phi(rad)$(NH/IH)
A1	0.05-0.35/0.05-0.3	1.57-1.60/1.57-1.60
A2	0.05-0.35/0.05-0.3	1.62-1.66/1.64-1.66
B1	0.05-0.35/0.45-0.55	1.57-1.60/1.57-1.60
B2	0.05-0.3/0.45-0.55	1.625-1.66/1.57-1.60
B3	0.05-0.35/0.45-0.55	1.62-1.66/1.64-1.66
B4	0.45-0.55/0.05-0.25	1.57-1.60/1.57-1.60

Table 5.10: The range of TM mixing parameters (θ and ϕ) that satisfies the KamLAND-Zen limit of effective Majorana neutrino mass.

Class	W(NH/IH)	X(NH/IH)	Y(NH/IH)	Z(NH/IH)
A1	0.03-0.1/ 0.03-0.1	0.02-0.1/ 0.02-0.1	0.01-0.05/ 0.03-0.05	0.005-0.1/ 0.01-0.09
A2	0.02-0.1/ 0.02-0.04	0.02-0.1/ 0.005-0.08	0.01-0.08/ 0.005-0.08	0.02-0.1/ 0.005-0.04
B1	0.005-0.06/ 0.02-0.05	0.005-0.1/ 0.005-0.04	0.005-0.1/ 0.01-0.08	0.02-0.1/ 0.01-0.08
B2	0.07-0.1/ 0.02-0.08	0.01-0.05/ 0.005-0.08	0.01-0.09/ 0.005-0.09	0.07-0.1/ 0.01-0.1
B3	0.01-0.08/ 0.01-0.06	0.005-0.1/ 0.01-0.1	0.005-0.08/ 0.01-0.08	0.03-0.08/ 0.01-0.08
B4	0.01-0.07/ 0.02-0.08	0.005-0.1/ 0.02-0.1	0.02-0.1/ 0.01-0.1	0.02-0.1/ 0.02-0.1

Table 5.11: The range of type II model parameters (in eV) that satisfies the KamLAND-Zen limit of effective Majorana neutrino mass.

5.6 Conclusion

The importance of texture zero neutrino mass and its phenomenological consequence has gained utmost significance in present-day research. In this context, two zero texture neutrino mass matrices are more relevant as they provide the minimal free parameters for precise study. We have performed a study of the Majorana neutrino mass matrix which has two independent zeros. As has been pointed out in several earlier works that seven out of fifteen patterns namely (A1, A2, B1-B4, C1) can survive the current experimental data at 3σ level. We tried to study the constraints of the allowed patterns of texture zero neutrino mass matrices in the framework of LRSM from low energy phenomena like NDBD and LFV. We have shown that one can obtain the desired two zero texture mass matrices by implementing an abelian discrete symmetric group $Z_8 \times Z_2$ in the framework of left-right symmetric model. The two zero textured neutrino mass matrix in our case is able to explain NDBD with the effective Majorana mass within the experimental limit propounded by ex-

periment (KamLAND-Zen). However, all the different allowed classes of two zero textures show different results for different neutrino mass hierarchies. Based on our results, having done a careful comparison of the plots obtained for different classes of two zero textures, it is seen that none of the cases totally disallows NDBD as far as the KamLAND-Zen limit is concerned irrespective of the mass hierarchies. However, the allowed range of the parameter space is constrained for the allowed experimental bounds of effective Majorana neutrino mass. We have considered six different allowed classes of two texture zero neutrino mass matrices satisfying TM mixing in our case. Again we have done an analysis of the model parameters (W, X, Y, Z) in our case which are heavily constrained for a very limited parameter space for some classes, specifically for the classes A2 (IH), B1(IH), B2 (NH) for some contributions of the model parameters which has been explained in numerical analysis. Thus we can say that the contributions from the type II SS in NDBD are relatively less for this class. Interestingly the present results ruled out B1, B4 classes (for both NH/IH) and A1 (NH), A2 (IH), B2 (IH) classes of two texture zero neutrino mass in explaining the experimentally allowed regions of charged lepton flavor violation whereas only the class B3 (NH/IH) is giving results within bounds for both the mass hierarchies. Again, the Majorana phases α and β are also constrained from both NDBD and LFV point of view. However, the sensitivity of NDBD experiments to the effective mass governing NDBD will probably reach around 0.05 eV in future experiments which might exclude or marginally allow some of the two zero texture patterns in the nearby future. However, here we have considered some random structures of the Dirac and Majorana mass matrix that leads to the two zero texture neutrino mass matrix. It would be interesting to study an in depth analysis for all the texture structures the Dirac and Majorana mass matrix that might lead to the zero textures in the neutrino mass matrix. We have left this study of the texture zero classes considering all the model parameters and its implications for all contributions of NDBD and LFV in the framework of LRSM for the next chapter that could lead to a more strong conclusion.

Bibliography

[1] De Salas, P. F., Forero, D. V., Ternes, C. A., Tortola, M. and Valle, J. W. F. Status of neutrino oscillations 2018: 3σ hint for normal mass ordering and improved CP sensitivity.*Phys Lett. B*, 782:633-640, 2018.

[2] Ishimori, H., Kobayashi, T., Ohki, H., Shimizu, Y., Okada, H. and Tanimoto, M. Non-Abelian discrete symmetries in particle physics. *Prog. Theor. Phys. Suppl.*, S183:1-163, 2010.

[3] Ludl, P. O. and Grimus, W. A complete survey of texture zeros in the lepton mass matrices. *JHEP*, 07:090, 2014.

[4] Frampton, P. H., Glashow, S.L and Marfatia, D. Zeroes of the neutrino mass matrix. *Phys Lett. B*, 536(1-2):79-82, 2002.

[5] Xing, Z. Z. Texture zeros and Majorana phases of the neutrino mass matrix. *Phys. Lett. B*, 530(1-4):159-166, 2002.

[6] Singh, M. Ahuja, G. and Gupta, M. Revisiting the texture zero neutrino mass matrices. *PTEP*, 2016(12):123B08, 2016.

[7] Ahuja, G. Texture Zero Mass Matrices And Their Implications. *What Comes Beyond the Standard Models*, 5(1):1, 2004.

[8] Meloni, D., Meroni, A. and Peinado, E. Two-zero Majorana textures in the light of the Planck results. *Phys. Rev. D*, 89(5):053009, 2014.

[9] Borah, M., Borah, D. and Das, M.K. Discriminating Majorana neutrino textures in light of the baryon asymmetry. *Phys. Rev. D*, 91(11):113008, 2015.

[10] Fritzsch, H., Xing, Z. Z. and Zhou, S.Two-zero textures of the Majorana neutrino mass matrix and current experimental tests. *JHEP*, 2011(9):83, 2011.

[11] Alcaide, J., Salvado, J. and Santamaria, A. Fitting flavour symmetries: the case of two-zero neutrino mass textures. *arXiv:1806.06785*, 2018.

[12] Zhou, S. Update on two-zero textures of the Majorana neutrino mass matrix in light of recent T2K, Super-Kamiokande and NOνA results. *Chinese Physics C*, 40(3):033102, 2016.

[13] Kaneko, S. and Tanimoto, M. Neutrino mass matrix with two zeros and leptogenesis. *Phys Lett.B*, 551(1-2):127-136, 2003.

[14] Dev, S., Radha R., and Singh, L.and Gupta, M. Two-texture zeros and near-maximal atmospheric neutrino mixing angle. *Pramana*, 86 (2):379-386, 2016.

[15] Nath, N., Ghosh, M. and Goswami, S. and Gupta, S. Phenomenological study of extended seesaw model for light sterile neutrino. *JHEP*, 2017(3):75, 2017.

[16] Agarwalla, S. K., Chatterjee, S. S., Petcov, S. T. and Titov, A. V. Addressing neutrino mixing models with DUNE and T2HK. *Eur. Phys. J. C*, 78 (4):286, 2018.

[17] Harrison, P. F. and Perkins, D. H. and Scott, W. G. Tri-bimaximal mixing and the neutrino oscillation data. *Phys. Lett. B*, 530 (1-4):167-173, 2002.

[18] Abe, K., et al. Observation of electron neutrino appearance in a muon neutrino beam. *Phys. Rev. Lett.*, 112(6):061802, 2014.

[19] An, F. P., Bai, J. Z., Balantekin, A. B., Band, H. R., Beavis, D., Beriguete, W., Bishai, M., Blyth, S., Boddy, K., Brown, R. L. Observation of electron-antineutrino disappearance at Daya Bay. *Phys. Rev. Lett.*, 108 (17):171803, 2012.

[20] Ahn, J.K., et al. Observation of reactor electron antineutrinos disappearance in the RENO experiment. *Phys. Rev. Lett.*,108 (19):191802, 2012.

[21] Rodejohann, W. and Xu, X. J. Trimaximal μ- τ reflection symmetry. *Phys. Rev. D*,96 (5):055039, 2017.

[22] Luhn, C. Trimaximal TM1 neutrino mixing in S4 with spontaneous CP violation. *Nucl. Phys. B*, S875 (1):80-100, 2013.

[23] Antusch, S., King, S. F., Luhn, C. and Spinrath, M. Trimaximal mixing with predicted $\theta 13$ from a new type of constrained sequential dominance. *Nucl. Phys. B*, 856 (2):328-341, 2012.

[24] Kumar, S. Unitarity constraints on trimaximal mixing. *Phys. Rev. D*, 82 (1):013010, 2010.

[25] Albright, C. H. and Rodejohann, W. Comparing trimaximal mixing and its variants with deviations from tri-bimaximal mixing. *Eur. Phys. J. C*, 62(3):599-608, 2009.

[26] Grimus, W. and Lavoura, L. A model for trimaximal lepton mixing. *JHEP*, 09:106, 2008.

[27] Gautam, R. R. Trimaximal mixing with a texture zero. *Phys. Rev. D*, 97(5):055022, 2018.

[28] Gautam, R. R. and Kumar, S. Zeros in the magic neutrino mass matrix. *Phys. Rev. D*, 94(3):036004, 2016.

[29] Dell'Oro, S., and Marcocci, S., Viel, M. and Vissani, F. Neutrinoless double beta decay: 2015 review. *Adv. High Energy Phys.*, 2016, 2016.

[30] Shirai, J. KamLAND-Zen Collaboration and others. Results and future plans for the KamLAND-Zen experiment. *J. Phys. Conf. Ser.*, 888(1):012031, 2017.

[31] Agostini, M., et al. Upgrade for Phase II of the Gerda experiment. *Eur. Phys. J. C*, 78(5):388, 2018.

[32] Albert, J.B., et al. Search for neutrinoless double-beta decay with the upgraded EXO-200 detector. *Phys. Rev. Lett.*, 120(7):072701, 2018.

[33] Senjanovic, G. and Mohapatra, R. N. Exact left-right symmetry and spontaneous violation of parity. *Phys. Rev. D*, 12(5):1502, 1975.

[34] Mohapatra, R. N. and Marshak, R. E. Local B- L symmetry of electroweak interactions, majorana neutrinos, and neutron oscillations. *Phys. Rev. Lett.*, 44(20):1316, 1980.

[35] Marshak, R.E., et al. Majorana neutrinos and low-energy tests of electroweak models. *Phys. Rev. D*, 24(5):1310, 1981.

[36] Abbas, M and Khalil, S. Neutrino masses, mixing and leptogenesis in TeV scale B- L extension of the standard model. *JHEP*, 2008(04):056, 2008.

[37] Dev, P. S. and Zhang, Y. Displaced vertex signatures of doubly charged scalars in the type-II seesaw and its left-right extensions. *JHEP*, 10:199, 2018.

[38] Ge, S. F., Lindner, M. and Patra, S. New physics effects on neutrinoless double beta decay from right-handed current. *JHEP*, 2015(10):77, 2015.

[39] Barry, J. and Rodejohann, W. Lepton number and flavour violation in TeV-scale left-right symmetric theories with large left-right mixing. *JHEP*, 2013(9):153, 2013.

[40] Awasthi, R. L., and Dev, P. S. B. and Mitra, M. Implications of the diboson excess for neutrinoless double beta decay and lepton flavor violation in TeV scale left-right symmetric model. *Phys. Rev. D*, 93(1):011701, 2016.

[41] Chakrabortty, J. and Devi, H. Z. and Goswami, S. and Patra, S. Neutrinoless double-β decay in TeV scale Left-Right symmetric models. *JHEP*, 08:008, 2012.

[42] Borah, D. and Dasgupta, A. Neutrinoless double beta decay in type I+II seesaw models. *JHEP*, 11:208, 2015.

[43] Patra, S. Neutrinoless double beta decay process in left-right symmetric models without scalar bidoublet. *Phys. Rev. D*, 87 (1):015002, 2013.

[44] Parida, M. K. and Patra, S. Left-right models with light neutrino mass prediction and dominant neutrinoless double beta decay rate. *Phys. Lett. B*, 718 (4-5):1407-1412, 2013.

[45] Bambhaniya, G., Dev, P. S. B and Goswami, S., Mitra, M. The scalar triplet contribution to lepton flavour violation and neutrinoless double beta decay in left-right symmetric model. *JHEP*, 04:046, 2016.

[46] Nemevek, M., and Senjanovic, G. and Tello, V. Connecting Dirac and Majorana neutrino mass matrices in the minimal left-right symmetric model. *Phys. Rev. Lett.*, 110 (15):151802, 2013.

[47] Ruiz, R. Lepton number violation at colliders from kinematically inaccessible gauge bosons. *Eur. Phys. J. C*, 77(6):375, 2017.

[48] Maiezza, A., Nemevek, M. and Nesti, F. Lepton number violation in Higgs decay at LHC. *Phys. Rev. Lett.*, 115(8):081802, 2015.

[49] Deppisch, F. F. Probing Leptonic Models at the LHC. *arXiv:1510.01302*, 2015.

[50] Helo, J. C. and Kovalenko, S. G. and Hirsch, M. Heavy neutrino searches at the LHC with displaced vertices. *Phys. Rev. D*, 89 (7):073005, 2014.

[51] Lam, C. S. Magic neutrino mass matrix and the Bjorken–Harrison–Scott parameterization. *Phys. Lett. B*, 640(5-6):260-262, 2006.

[52] Singh, M. and Gautam, R. R. Exploring texture two-zero Majorana neutrino mass matrices with the latest neutrino oscillation data. *Springer Proc. Phys.*, 174:323-327, 2016.

[53] Dev, S., Kumar, S., Verma, S. and Gupta, S. CP violation in two zero texture neutrino mass matrices. *Phys. Lett. B*, 656(1-3):79-82, 2007.

[54] Cirigliano, V., Kurylov, A., Ramsey-Musolf, M. J. and Vogel, P. Lepton flavor violation without supersymmetry. *Phys. Rev. D*, 70:075007, 2004.

[55] Calibbi, L. and Signorelli, G. Charged lepton flavour violation: an experimental and theoretical introduction. *arXiv:1709.00294*,2017.

[56] Bernstein, R. H. and Cooper, P. S. Charged lepton flavor violation: an experimenter's guide. *Phys. Rept.*, 532(2):27-64, 2013.

[57] Perez, P. F. and Murgui, C. Lepton flavor violation in left-right theory. *Phys. Rev. D*, 95(7):075010, 2017.

[58] Deppisch, F. F., Gonzalo, T.E. and Patra, S., Sahu, N. and Sarkar, U. Double beta decay, lepton flavor violation, and collider signatures of left-right symmetric models with spontaneous D-parity breaking. *Phys. Rev. D*, 91(1):015018, 2015.

[59] Baldini, A. M., et al. [MEG collaboration]. Search for the lepton flavour violating decay$\mu \to e\gamma$ with the full dataset of the MEG experiment. *Eur. Phys. J. C*, 76(8):434 (2016).

[60] Mitra, M., Ruiz, R., Scott, D. J. and Spannowsky, M. Neutrino jets from high-mass W R gauge bosons in TeV-scale left-right symmetric models. *Phys. Rev. D*, 94(9):095016, 2016.

[61] Gando, A., et al. Search for Majorana Neutrinos near the Inverted Mass Hierarchy Region with KamLAND-Zen. *Phys. Rev. Lett.*, 117:082503, 2016.

[62] Tello, V., Nemevek, M., Nesti, F. and Senjanovic, G. and Vissani, F. Left-right symmetry: from the LHC to neutrinoless double beta decay. *Phys. Rev. Lett.*, 106(15):151801, 2011.